



**MARINHA DO BRASIL**  
**INSTITUTO DE ESTUDOS DO MAR ALMIRANTE PAULO MOREIRA**  
**UNIVERSIDADE FEDERAL FLUMINENSE**  
**PROGRAMA ASSOCIADO DE PÓS-GRADUAÇÃO EM BIOTECNOLOGIA MARINHA**

**THIAGO DA SILVA MATOS**

**MÉTODOS DE IMAGEAMENTO E ANÁLISE DO PLÂNCTON PARA  
MONITORAMENTO DAS VARIAÇÕES TEMPORAIS EM MULTIPLAS ESCALAS.**

**Arraial do Cabo / RJ**  
**2023**



**MARINHA DO BRASIL**

**INSTITUTO DE ESTUDOS DO MAR ALMIRANTE PAULO MOREIRA**

**UNIVERSIDADE FEDERAL FLUMINENSE**

**PROGRAMA ASSOCIADO DE PÓS-GRADUAÇÃO EM BIOTECNOLOGIA MARINHA**

**THIAGO DA SILVA MATOS**

**MÉTODOS DE IMAGEAMENTO E ANÁLISE DO PLÂNCTON PARA  
MONITORAMENTO DAS VARIAÇÕES TEMPORAIS EM MULTIPLAS ESCALAS.**

Tese apresentada ao curso de Pós-graduação em Biotecnologia Marinha, Instituto de Estudos do Mar Almirante Paulo Moreira e à Universidade Federal Fluminense, como requisito parcial a obtenção do título de Doutor em Biotecnologia Marinha. Área de concentração Biologia Marinha. Linha de Pesquisa: Bio-Recursos Marinhos.

Orientador: Dr. Lohengrin Dias de Almeida Fernandes

**Arraial do Cabo - RJ**

**2023**

## FICHA CATALOGRÁFICA

M433m Matos, Thiago da Silva

Métodos de imageamento e análise do plâncton para monitoramento das variações temporais em multiplas escalas / Thiago da Silva Matos. – Arraial do Cabo, 2023.

79 f.: il.; 30 cm.

Orientador: Lohengrin Dias de Almeida Fernandes.

Tese (Doutorado) – Instituto de Estudos do Mar Almirante Paulo Moreira e Universidade Federal Fluminense - IEAPM/UFF, Programa Associado de Pós-Graduação em Biotecnologia Marinha, Arraial do Cabo, 2023.

1. Ecotaxa 2. Biodiversidade. 3. Biotecnologia Marinha  
I. Fernandes, Lohengrin Dias de. II. Título.

CDD:660.6

**THIAGO DA SILVA MATOS**

**MÉTODOS DE IMAGEAMENTO E ANÁLISE DO PLÂNCTON PARA  
MONITORAMENTO DAS VARIAÇÕES TEMPORAIS EM MULTIPLAS ESCALAS.**

Tese apresentada ao curso de Pós-Graduação em Biotecnologia Marinha, Instituto de Estudos do Mar Almirante Paulo Moreira e à Universidade Federal Fluminense, como requisito parcial a obtenção do título de Doutor em Biotecnologia Marinha. Área de concentração Biologia Marinha. Linha de Pesquisa: Bio-Recursos Marinhos.

**BANCA EXAMINADORA**

---

Prof. Dr. Lohengrin Dias de Almeida Fernandes (Orientador)  
IEAPM – Instituto de Estudos do Mar Almirante Paulo Moreira

---

Prof. Dr. Sávio Henrique Calazans  
IEAPM – Instituto de Estudos do Mar Almirante Paulo Moreira

---

Prof. Dr. Fábio Contrera Xavier  
IEAPM – Instituto de Estudos do Mar Almirante Paulo Moreira

---

Prof. Dr. Eduardo Vianna de Almeida  
UFRJ – Universidade Federal do Rio de Janeiro

---

Prof. Dr. José Eduardo Arruda Gonçalves  
IEAPM – Instituto de Estudos do Mar Almirante Paulo Moreira

---

Prof. Dr. Eduardo Barros Fagundes Netto  
IEAPM – Instituto de Estudos do Mar Almirante Paulo Moreira

**Arraial do Cabo / RJ, 31 de julho de 2023.**

Dedico esta tese a todo ser humano, que não se deixa abater pelas lutas e dificuldades, e tem seus sonhos realizados e sua história transformada através da fé em Deus e da educação.

## AGRADECIMENTOS

À Deus, por sempre me conduzir por caminhos difíceis, mas de resiliência, proporcionando crescer em graça e em conhecimento.

Ao meu Orientador Dr. Lohengrin Dias de Almeida Fernandes, agradeço a Deus por sua vida, por ter aceitado me orientar e incansavelmente dedicou seu tempo, atenção, e conhecimento na orientação deste trabalho, sem medir esforços ajudou a romper as inúmeras dificuldades. Em todo tempo se ocupou em ensinar, orientar, e algumas vezes quando precisei, foi um grande conselheiro, sempre demonstrando amizade comigo e com todos no laboratório. Sempre deu mais suporte do que cobrou, se preocupando no aprendizado e apropriação dos conhecimentos necessários para minha formação profissional.

A meus pais por toda dedicação, amor e carinho, em especial à minha mãe, que sempre me incentivou sem ao menos saber e entender o que eu estudava, mas confiava ser um passo importante e especial na minha vida.

À minha esposa, por sempre incentivar e entender os momentos de dedicação exclusiva ao trabalho, demonstrando paciência e sabedoria através de palavras, atenção, e carinho, ressaltando o quanto era importante o meu trabalho.

Ao meu Filho Benjamin, um verdadeiro presente de Deus no meio da pandemia, junto de um doutorado, para muitos um péssimo momento para ser pai, mas foi o melhor momento, pois ele foi um instrumento de Deus para me impulsionar a não desistir, me ensinou o que é ser resiliente.

Aos meus irmãos, que direta ou indiretamente sempre participaram das minhas conquistas, sempre incentivando e ajudando, Hênio, Matheus, Gabriel, Maryana, e todos os meus familiares (em especial dona Sheila e seu Roberto), obrigado.

Aos meus amigos Fábio Contrera e Laís Naval, vocês participaram muito dessa conquista, desse momento importante na minha formação, minha gratidão.

A minha amiga Wanessa Stida, representando todos os amigos bolsistas do IEAPM, por sua amizade e companheirismo, tornando dias cansativos no laboratório em momentos de muito trabalho, porém de leveza na alma em fazer o que gostamos com pessoas que nos apoiam.

Aos amigos João Laudares, Bruna Figueiredo, por companheirismo e amizade. A minha amiga Aline Câmara e meu grande amigo Marcio Tenório, que mesmo distante mantiveram o carinho e a amizade.

À minha querida amiga Wanda Ribas, por dedicar seu precioso tempo em me ensinar um pouco dos conhecimentos taxonômicos, e sempre disposta a tirar qualquer dúvida na identificação de copépodes.

A todos os amigos da igreja e pastores por todo companheirismo e auxílio, palavras de incentivos e orações.

Ao sensei Paulo Pinto e todos os amigos do karatê, por todo incentivo e companheirismo.

A todos os amigos professores de escolas públicas e privadas que trabalhei, em especial meus amigos, Fabiano Chico, Otávio, Marildo, Gastão, Dávila, Tia Lúcia, Isalira, Roseclea (in memória).

Aos professores (biólogos) que desde o ensino fundamental e médio, e no período que fui estagiário na secretaria de meio ambiente, me fizeram despertar para o estudo da vida: Renato Abreu, Marlon, Carlinhos, Fátima, Sheila, Paulo cordeiro, David Barreto, Jean Carlos e Everaldo Cunha.

Ao PPGBM, em especial ao coordenador, Dr. Ricardo Coutinho, a Dra. Maria Helena, chefe do Departamento de Pós-graduação, e a todos os professores do curso de pós-graduação em Biotecnologia Marinha. A todos os amigos do Departamento de Biotecnologia Marinha, pelo suporte necessário à realização deste trabalho. Em especial à Divisão de Biotecnologia Aplicada, Dr. Lohengrin Fernandes, Tenente Laura Moura, Márcio Abreu, Carolina S. dos Reis, Andressa Cláudio, Vanessa Trindade, Ana Carolina Luz, e ao João Vítor.

Ao projeto Mission Atlantic, que financiou o pagamento mensal das bolsas de estudo, e pelo apoio na minha participação em um congresso na Espanha, custeando toda viagem, que me proporcionou apresentar um trabalho na conferência ECSA 59.

Aos membros da banca, Dr. Eduardo Vianna (UFRJ), Dr. Sávio Henrique Calazães (IEAPM), Dr. José Eduardo Arruda (IEAPM), Dr. Fábio Contrera Xavier (IEAPM), Dr. Eduardo Fagundes Netto (IEAPM) por gentilmente aceitarem o convite.

À Marinha do Brasil e ao Instituto de Estudos do Mar Almirante Paulo Moreira por ter cedido sua estrutura para que esse estudo fosse realizado.

## SUMÁRIO

<b>LISTA DE SIGLAS E ABREVIATURAS.....</b>	<b>x</b>
<b>ÍNDICE DE FIGURAS.....</b>	<b>xii</b>
<b>ÍNDICE DE TABELAS.....</b>	<b>xv</b>
<b>RESUMO .....</b>	<b>xvi</b>
<b>ABSTRACT .....</b>	<b>xviii</b>
<b>INTRODUÇÃO GERAL .....</b>	<b>19</b>
<b>OBJETIVOS .....</b>	<b>22</b>
Objetivos específicos.....	22
<b>CAPÍTULO I: .....</b>	<b>23</b>
EFFECT OF TURBIDITY ON SEMI-AUTOMATIC ANALYSIS OF COPEPOD SIZE AND ABUNDANCE DISTRIBUTION IN THE WATER COLUMN .....	23
ABSTRACT .....	23
INTRODUCTION.....	24
METHODS .....	26
Study site .....	26
The Light Frame On-sight Key Species Investigation (LOKI).....	27
RESULTS.....	30
Images of interest .....	30
Image cropping .....	31
Binarization performance in discriminating one single copepod .....	33
Size of the copepod .....	34
Enumeration algorithm.....	35
DISCUSSION .....	36
ACKNOWLEDGEMENTS.....	39
FUNDING.....	39
REFERENCES .....	39



<b>CAPÍTULO II:</b> .....	<b>44</b>
NEW DIVERSITY INDEX TO ESTIMATE THE PLANKTONIC ASSEMBLAGE WITH IMAGES ON THE ECOTAXA WEBSITE .....	44
ABSTRACT .....	44
INTRODUCTION .....	45
MATERIAL AND METHODS .....	47
Study Site .....	47
RESULTS .....	48
CHANGE IN THE ASSEMBLAGE DIVERSITY .....	49
DISCUSSION .....	51
ACKNOWLEDGMENTS .....	53
CONFLICT OF INTEREST .....	53
REFERENCES .....	53
<b>CAPÍTULO III</b> .....	<b>56</b>
EARLY WARNING INDICATORS OF SHIFTS IN THE PLANKTON ASSEMBLAGE IN UPWELLING ECOSYSTEMS .....	56
Abstract .....	57
INTRODUCTION .....	57
MATERIAL AND METHODS .....	59
Study site .....	59
Plankton image acquisition .....	61
Time series analyses .....	62
RESULTS .....	63
Decadal change in temperature and salinity .....	63
Temporal change in the plankton assemblage .....	66
DISCUSSION .....	69
ACKNOWLEDGMENTS .....	71
FUNDING .....	71

CONFLICT OF INTEREST .....	71
AUTHOR CONTRIBUTION .....	71
REFERENCES .....	71
<b>CONSIDERAÇÕES FINAIS.....</b>	<b>79</b>
<b>REFERÊNCIAS BIBLIOGRÁFICAS.....</b>	<b>80</b>

### LISTA DE SIGLAS E ABREVIATURAS

ACAS – Água Central do Atlântico Sul

AC – Água Costeira

AT – Água Tropical

CB – Corrente do Brasil

ESD – Equivalent Spherical Diameter

FlowCAM – Flow Cytometer and Microscopy

°C - Graus Celsius

µm - Micrômetro

Org.m<sup>-3</sup> - Organismos por metro cúbico

PELD-RECA – Pesquisas Ecológicas de Longa Duração da Ressurgência de Cabo Frio

VSP – Visual Spreadsheet

ClaSup – Clorofila a da superfície

TemSup – Temperatura de superfície

SalSup - Salinidade de superfície

DOSup - Oxigênio dissolvido

pHSup - PH da superfície

ClaBot – Clorofila a de fundo

TemBot – Temperatura de fundo

SalBot - Salinidade de fundo

DOBot – Oxigênio dissolvido no fundo

pHBot - pH de fundo

WWeight - Biomassa peso úmido

DWeight - Biomassa peso seco

CopSum - Soma dos copepodes  
Calanoida - Grupo Calanoida  
Tturb - Temora turbinata  
CopCut – Corte dos Copepoda  
Corycaeus - Grupo Ceyceus  
Eacutif - Euterpina acutifrons  
Mgracil - Microsetella gracilis  
Oithona - Oithona  
Ohebes - Oithona hebes  
Oncaea - Oncaea  
Pavir - Penilha avirostris  
Ppoly – Podon polyfenoides  
Espin - Espinifera  
HoloSum - Soma do Holoplancton  
Cirrip - Cirripédia  
MeroSum – Soma do Meroplancton  
OTU – Unidade Taxonômica Operacional  
CFUS – Sistema de Ressurgência do Cabo Frio  
ZOPACAS – Zona de Paz e cooperação do Atlântico Sul  
SWAO – Sudoeste do Atlântico Sul  
VIF – Fator de Variância  
RDA – Análise de Redundância  
Kb – Kilo byte  
IDI- Image Diverse Index  
NTU – Unidade Nefelometrica de Turbidez

## ÍNDICE DE FIGURAS

Figure 1. Map representing the collection points: one with high turbidity near the outfall, and the other with less turbidity farther away. ....	27
Figure 2. Example of vertical profile of temperature (°C) and pressure (mbar) during a LOKI haul. The red dotted square highlights the vertical haul from near the bottom back to the surface. ....	28
Figure 3. Steps of the treatment of the images. A) Original vignette, automatically cropped by the LOKI system. B) Resulting binarization of vignette exemplified by the “Default” algorithm C) Resulting of the contour detection algorithm used in the copepod counting and measurement. .	29
Figure 4. Vertical profiles of temperature (°C) and pressure (mbar) during the two LOKI hauls at the point with high turbidity (A, site 1) and low turbidity (B, site 2). The red dotted rectangles highlight the accepted vertical haul from which images were analyzed .....	31
Figure 5. Laser-Optical Plankton Counter (LOPC) profile from site 1 (position 1) to site 2 (position 7) after seven sequential deployments showing the gradient of suspended particles. The scale of particle counts (Single Element Plankton) is on the right. ....	31
Figure 6. Distribution of size classes of the files. ....	32
Figure 7. Examples of in situ photography (grayscale) and the corresponding histogram showing more suspended sediments (‘noise’) around the copepod in site 1 (A) than in the copepod in site 2 (B). ....	33
Figure 8. Performance of the 16 binarization methods (A-Default, B-Huang, C-Intermodes, D-IsoData, E-Li, F-MaxEntropy, G-Mean, H-MinError, I-Minimum, J-Moments, K -Osu, L-Percentile, M-RenyiEntropy, N-Shanbhag, O-Triangle, P-Yen) available on ImageJ, compared to the manual method. ....	34
Figure 9. Fragmentation of copepod’s body after binarization by ‘default’, ‘Otsu’, and ‘Minimum’ algorithms, compared to the actual copepod contour (manual). The number of fragments is signaled in red. ....	34
Figure 10. Relationship between the copepod’s body area as estimated from 16 automatic algorithms and the actual area manually measured. The linear regression equation and the R2 for each algorithm are shown inside the scatterplot. ....	35
Figure 11. Comparison between two points with different turbidity conditions in the treatment using the four algorithms. ....	36
Figure 12. EcoTaxa website interface ( <a href="https://ecotaxa.obs-vlfr.fr/">https://ecotaxa.obs-vlfr.fr/</a> ). The researcher can browse the database along a taxonomic tree (as in the example on the left of the image) or filter the images according to sampling criteria (location, time, depth) or even morphological characteristics	

such as (size, chlorophyll a, among others). Fast identification of a large set of images is performed by combining machine learning and human validation. ....	48
Figure 13. Estimated monthly variation between 1998 and 2015 in plankton class diversity. The blue arrows represent peaks of high diversity. ....	50
Figure 14. Annual average temperature variation (solid circles = surface; empty circles = background) and average class diversity.....	51
Figure 15. Annual mean salinity variation (solid circles = surface; empty circles = bottom) and mean class diversity.....	51
Figure 16. Monthly change in plankton class diversity calculated for the pooled months from 1998 to 2015.....	51
Figure 17. Monthly composite Chlorophyll concentration (MODIS Aqua L3 4km resolution) in the South Atlantic Ocean during January 2003 (Ocean Color, NASA). The Cabo Frio Upwelling System (CFUS, top panel) delimits the northern boundary of the South Brazilian Shelf in the southwestern South Atlantic Ocean (SWAO), a highly-productive ecosystem on the west that contributes to the South Atlantic primary production along with the Benguela System (BS) on the east. ....	60
Figure 18. Decadal (1950-2023) change in the sea surface temperature (A) and salinity (B) in the CFUS. ....	64
Figure 19. Wavelet transformation of temperature (A) and salinity (B), wavelet coherence (C), and monthly variation (seasonal) of temperature (D) and salinity (E) in the CFUS. ....	65
Figure 20. Annual average of dissolved oxygen (A), pH (B), temperature (C), ammonia (D), phosphate (E), salinity (F), nitrite+nitrate (G), and first two Principal Component axis. ....	66
Figure 21. Scatterplots, histograms and correlation between the annual average of phytoplankton (Diatom, Dinoflagellates, and Chlorophyll-a) and zooplankton (Dry Weight, Copepod, and Cladoceran). * $p < 0.5$ , ** $p < 0.1$ , *** $p < 0.01$ . ....	66
Figure 22. Scatterplot of dimensions 1 and 2 from the Redundancy Analysis in CFUS. ....	68
Figure 23. Annual average (horizontal line) of phytoplankton (A-C; Chlorophyll-a, Dinoflagellates, Diatoms) and zooplankton normalized-density (D-E; Dry Weight, Copepods, Cladocerans) $\pm$ the 25th and 75th percentiles (lower and upper hinges respectively), $\pm 1.5*$ interquartile range (lower and upper whiskers respectively), raw data (black dots), and the linear model (dashed blue line).....	68
Figure 24. Ranked yearly distribution of quintiles of phytoplankton and zooplankton data (coloured scale) with superimposed scores of years in the first dimension of RDA (scales on the right).....	69



**ÍNDICE DE TABELAS**

Table 1. Turbidity and particle concentration at the two sites. ....	30
Table 2. Comparison of the performance of LOKI segmentation algorithm in cropping vignettes under high and low turbidity. ....	32
Table 3. Statistics of the above grayscale images (vignettes) from site 1 (with high ‘noise’) and site 2 (with low ‘noise’). ....	33
Table 4. Comparison of the number of copepods estimated visually by an expert (visual inspection, 100%) and automatically following four algorithms elaborated in ImageJ. ....	36
Table 5. The 43 plankton categories used to infer the class diversity index. ....	49
Table 6. Variance Inflation Factors (VIF) of variables included in the model before (Round 1) and after (Round 2) remotion of collinearity. ....	66

## RESUMO

Parte do planeta Terra é coberto por oceanos, com sua biodiversidade marinha composta principalmente por organismos planctônicos e sua grande relevância para a humanidade na produção de alimento e oxigênio. Estudar esses organismos a longo prazo permite entender alterações no ecossistema. Neste escopo, o presente trabalho teve os seguintes objetivos: desenvolver um protocolo de classificação e contagem automática de plâncton nos sistemas de imageamento Loki e FlowCam; desenvolver um novo índice de diversidade para trabalhar com as classes de imagens no website ECOTAXA; avaliar possíveis correlações entre variações temporais na estrutura da comunidade (betadiversidade-ECOTAXA); e aplicar os parâmetros de abundância e tamanho médio dos organismos como indicadores de mudanças nos ciclos naturais de variações temporais e sazonais das populações do holoplâncton. Para realização do estudo descrito no primeiro capítulo, as imagens foram obtidas no dia 27 de novembro de 2015, com o *Lightframe On-Sight Keyspecies Investigation System* (LOKI), e nos dois outros capítulos, foram obtidas imagens, em laboratório, de amostras coletadas semanalmente entre os anos de 1998 e 2015, na Ilha de Cabo Frio em Arraial do Cabo, RJ. No primeiro capítulo, um dos algoritmos testados para caracterização automática foi melhor, estatisticamente, pelo teste de dissimilaridade, com taxa de acerto de 96%. No segundo capítulo, os resultados mostraram uma variação na diversidade de classes de imagens ao longo do tempo, entre 0,38 e 2,04 ( $\pm 0,28SD$ ) bits.class-1. Também foi observado um aumento anual da temperatura acompanhado do aumento da diversidade. No terceiro capítulo, A mudança entre um regime dominante de diatomáceas para um dinoflagelado indica as respostas distintas que esses organismos têm a certas condições ambientais. As espécies de dinoflagelados, ao contrário das diatomáceas, são especialistas em ecossistemas com maiores taxas de salinidade e temperatura e baixas concentrações de nutrientes. Diferentemente dos grupos zooplanctônicos – copépodes e cladóceros – os dinoflagelados são considerados tipos oportunistas de fitoplâncton que apresentam tendências a mudanças abruptas em ecossistemas como o fenômeno da ressurgência.

**Palavras-chave:** Semiautomática, ECOTAXA, Biodiversidade, mudanças climáticas, temperatura, variações temporais.





## ABSTRACT

Part of planet Earth is covered by oceans, with its marine biodiversity composed mainly of planktonic organisms and its great relevance for humanity in the production of food and oxygen. To study these organisms in a long term allows to understand changes in the ecosystem. In this scope, the present work had the following objectives: to develop a protocol for automatic classification and counting of plankton in the Loki and FlowCam imaging systems; to develop a new diversity index to work with classes of images on the website ECOTAXA; to evaluate possible correlations between temporal variations in the structure of a community (betadiversity-ECOTAXA); and to apply the parameters of abundance and average size of the organisms as indicators of changes in the natural cycles of temporal and seasonal variations of populations of the holoplankton. To carry out the study described in the first chapter, the images were obtained on November 27, 2015, with the Lightframe On-Sight Keyspecies Investigation System (LOKI), and in the two other chapters, laboratory images were obtained from samples collected weekly between the years of 1998 and 2015, on Cabo Frio Island in Arraial do Cabo, RJ. In the first chapter, one of the algorithms tested for automatic characterization was statistically better by the dissimilarity test, with a success rate of 96%. In the second chapter, the results showed a variation in the diversity of image classes over time, between 0.38 and 2.04 ( $\pm 0.28SD$ ) bits.class<sup>-1</sup>. An annual increase in temperature was also observed, accompanied by an increase in diversity. In the third chapter, the Shift from a diatom dominant to a dinoflagellate regime indicates the distinct responses these organisms have to certain environmental conditions. Dinoflagellate species, unlike diatoms, are specialists in ecosystems with higher salinity and temperature and low concentrations of nutrients. Unlike zooplanktonic groups – copepods and cladocerans – dinoflagellates are considered opportunistic types of phytoplankton that tend to abrupt changes in ecosystems such as the upwelling phenomenon.

**Keywords:** Climate changes, ECOTAXA, Semi-automatic classification, Biodiversity Temperature, Temporal variation4s.

## INTRODUÇÃO GERAL

Os oceanos recobrem aproximadamente 75% da superfície da Terra. Esse número ressalta sua relevância para a humanidade, sendo o oceano responsável por boa parte da matéria orgânica produzida a partir da energia luminosa: 50% da Produção Primária Global (DANOVARO *et al.*, 2011). Esses dados evidenciam a importância dos oceanos para a vida e ressaltam a necessidade de monitorar ocasionais mudanças e seus efeitos no bioma marinho.

Neste escopo, estudar o ambiente marinho, sua biodiversidade e dinâmica trófica, permite compreender os fenômenos oceânicos e aperfeiçoar técnicas de monitoramento ambiental. Mudanças nos oceanos, sejam antrópicas ou naturais, afetam direta ou indiretamente alguns organismos. Dentre os organismos com potencial para indicar mudanças ambientais, temos os organismos planctônicos. Esses organismos pertencem a diversos grupos taxonômicos de diferentes tamanhos, são responsáveis por parte do nosso oxigênio disponível e compõem a base da cadeia alimentar marinha. Eles possuem grande capacidade natatória, que, na maioria das vezes, é limitada pelas barreiras físicas como as correntes marinhas (BOLTOVSKOY, 1981; SCHMID *et al.*, 2016).

Em termos de abundância, biomassa e biodiversidade, os copépodes ocupam a posição de organismos mais importantes do mesozoplâncton marinho, mesmo as classes de menor escala de tamanho, sendo elo intermediário entre a produção primária e outros níveis tróficos e tendo papel fundamental na dinâmica do ecossistema e no ciclo global do carbono (HARRIS *et al.*, 2000; HIRCHE *et al.*, 2012). A classificação dos copépodes é baseada na tagmose do corpo, na segmentação e na armadura dos apêndices cefálicos e torácicos. O corpo é dividido em uma porção anterior – o prossoma e uma porção posterior – o urossoma ou abdome, que é desprovido de apêndices (BONECKER, S. L. C., 2006). O urossoma, porção posterior do copépoda, é composta pelos somitos genitais e pela furca (BOLTOVSKOY, 1981). Quanto a distinção entre macho e fêmea, esses microcrustáceos apresentam dimorfismo sexual (BRADFORD-GRIEVE *et al.*, 1999). Além disso, são organismos que possuem hábitos bastante diversificados na alimentação, podendo ser onívoros, herbívoros, carnívoros ou detritívoros. (TURNER, 2004; CALBET, 2008).

Compreender a dinâmica espacial e temporal dos organismos planctônicos e como eles interagem tem sido foco principal no estudo da ecologia do plâncton. Dimensionar a dinâmica da produção secundária de copépodes é essencial para compreender o papel

do zooplâncton como fonte de matéria e energia para níveis tróficos mais altos nos ecossistemas marinhos (HIRST and BUNKER, 2003). As condições ambientais locais, as fontes de alimento e as interações na cadeia trófica definem a dinâmica e a estrutura das comunidades planctônicas, as quais podem ser usadas como um diagnóstico, por exemplo, do status da produção primária do bioma marinho. De acordo com BRANDINI *et al.* (1997), alterações em todos os níveis tróficos do ecossistema marinho podem ser observadas a partir de mudanças na comunidade planctônica.

Diante do cenário atual e dos avanços dos estudos ecológicos, é possível observar o desenvolvimento de diferentes equipamentos de aquisição de imagens nas últimas décadas, dentre eles várias tecnologias capazes de registrar imagens de organismos zooplanctônicos, desde sistemas adaptados a bancada do laboratório, como o Flow Cytometer e Microscope 'FlowCAM' e o 'ZooScan' (GROSJEAN *et al.*, 2004; GORSKY *et al.*, 2010), e também sistemas de aquisição de imagens *in situ*, como o 'Vídeo Plankton Recorder' (VPR - TANG *et al.*, 1998; DAVIS *et al.*, 2004), o 'Underwater Vision Profiler' (UVP), o 'Zooplankton Visualization System' (ZOOVIS), o 'Lightframe On-Site Keyspecies Investigation System' (LOKI), o 'Shadow Image Particle Profiling Evaluation Recorder' (SIPPER - LUO *et al.*, 2004), FlowCytobot (SOSIK and OLSON, 2007) e o '*In Situ* Ichthyoplankton Imaging System' (ISIIS) (BI *et al.*, 2015).

Segundo HENZLER *et al.* (2010), ter um método eficiente para identificar com precisão e contabilizar organismos marinhos permitiria à comunidade científica acessar amostras armazenadas em coleções de plâncton e a realização de novos projetos em larga escala espacial e temporal. Para realizar a classificação dos organismos com imagens são utilizadas técnicas matemáticas, que são aplicadas às imagens obtidas (GONZALEZ *et al.*, 2004).

Este trabalho traz no primeiro capítulo tecnologias de análise e classificação automática de zooplâncton como ferramenta prática para economizar tempo e viabilizar respostas mais rápidas a situações ambientais.

O segundo capítulo apresenta um novo índice de diversidade, aplicado a imagens capturadas por diversos equipamentos e traz resultados a respeito da diversidade de organismos na região da Ressurgência do Cabo Frio com este novo índice.

O terceiro capítulo traz a distribuição temporal da assembleia zooplanctônica durante eventos de ressurgência e subsidência ao longo dos anos. A abundância, biomassa e tamanho dos copépodes foram analisados frente às variáveis ambientais de temperatura, salinidade, oxigênio dissolvido, ph e concentração de clorofila-a. Também

ressalta a importância de acompanhar as mudanças climáticas, procurando na distribuição dos organismos algum em especial como indicador de tais mudanças.

O trabalho de pesquisa “Métodos de Imageamento e Análise do Plâncton para Monitoramento das Variações Temporais em Múltiplas Escalas” é vinculado e financiado pelo projeto “Mission Atlantic”, um projeto envolvendo vários países e instituições de pesquisa, em prol de estudar a saúde do Oceano Atlântico.

Esse projeto é uma ação decorrente do Programa de Pesquisas Ecológicas de Longa Duração da Ressurgência de Cabo Frio (PELD-RECA) que teve como objetivo o monitoramento de longo prazo das interferências antrópicas no ecossistema da ressurgência de Cabo Frio.

## OBJETIVOS

Esse projeto tem o objetivo geral de desenvolver tecnologia de monitoramento e diagnóstico das variações nas populações planctônicas do Atlântico, considerando os processos produtivos associados à ressurgência.

### **Objetivos específicos**

Com base na hipótese de que algumas populações de organismos planctônicos podem ser indicadoras de alterações no ecossistema marinho, este trabalho tem como objetivos específicos:

- a) Desenvolver um protocolo de contagem, classificação e análise de partículas marinhas (plâncton + tripton(abioseston)) para monitoramento de longo prazo.
- b) Desenvolver um novo índice de diversidade para aplicar com imagens previamente classificadas.
- c) Avaliar a dependência da composição da comunidade (betadiversidade-ECOTAXA) em relação aos parâmetros temperatura e salinidade, como indicadores de alterações de status do ecossistema.
- d) Aplicar os parâmetros de abundância e tamanho médio dos organismos planctônicos como indicadores de mudanças nos ciclos naturais de variações temporais das populações do holoplâncton (Copepoda e Cladocera).

**CAPÍTULO I:**

**Artigo submetido na Revista:** Brazilian Archives of Biology and Technology

**EFFECT OF TURBIDITY ON SEMI-AUTOMATIC ANALYSIS OF COPEPOD SIZE AND ABUNDANCE DISTRIBUTION IN THE WATER COLUMN**

Thiago da Silva Matos<sup>1</sup>, Carolina Siqueira dos Reis<sup>1</sup>, Laura de Andrade Moura<sup>2</sup>, Márcio Abreu<sup>2</sup>, Ricardo Coutinho<sup>1,2</sup>, Lohengrin Fernandes<sup>1,2</sup>

T.M.: [ORCID®](#) 0000-0002-9390-7669

C.R.: [ORCID®](#) 0000-0003-1584-0988

M.A.: [ORCID®](#) 0009-0006-0633-9429

L.M.: [ORCID®](#) 0000-0003-0002-9981

R.C.: [ORCID®](#) 0000-0001-5430-2176

L.F.: [ORCID®](#) 0000-0002-8579-2363

<sup>1</sup>IEAPM/UFF Marine Biotechnology Post-Graduate Program.

<sup>2</sup>Instituto de Estudos do Mar Almirante Paulo Moreira.

(Instituto de Estudos do Mar Almirante Paulo Moreira, Departamento de Biotecnologia Marinha, Divisão de Biotecnologia Aplicada. Rua Kioto, 253; Praia dos Anjos; 28930-000 - Arraial do Cabo, RJ – Brasil).

**TSM** e-mail: [biologo.thiagomatos@gmail.com](mailto:biologo.thiagomatos@gmail.com)

**CSR** e-mail: [carolinasreis@gmail.com](mailto:carolinasreis@gmail.com)

**LAM** e-mail: [laura\\_moura@outlook.com](mailto:laura_moura@outlook.com)

**MA** e-mail: [marcio-abreu@hotmail.com](mailto:marcio-abreu@hotmail.com)

**RC** e-mail: [rcoutinhosa@yahoo.com](mailto:rcoutinhosa@yahoo.com)

**LDAF** e-mail: [lohengrin.fernandes@gmail.com](mailto:lohengrin.fernandes@gmail.com)

**\*CORRESPONDING AUTHOR**

Thiago da Silva Matos

[biologo.thiagomatos@gmail.com](mailto:biologo.thiagomatos@gmail.com)

Running head: Matos *et al.*: Algorithm of semi-automatic analysis of copepods

**ABSTRACT**

Automated image systems to characterize aquatic organisms improve research and enable fast response to environmental risk situations. On November 2015, a dam in Mariana - MG (Brazil) collapsed and led to the disposal of mud tailings from the mining process to the Doce River. The accident resulted in incalculable damage to surrounding communities and to the environment. The mud increased water turbidity, an essential condition to the functioning of the image analysis systems, and directly affected the characterization of the organisms. To get a quick response to risk environmental situations, the aim of this work was to develop an algorithm to characterize and classify copepods by their size and area using images sampled by the LOKI System. The tests were carried out in different turbidity level points of the Doce River. The algorithm reduced about 50% of the amount of raw data in some samples. Four algorithms were tested for automatic characterization and compared with manual treatment. Statistically, one of the algorithms was the best by the dissimilarity test, with a successful rate of 96%. The results showed that this algorithm has a potential to improve the classification accuracy of copepods using images.

**Keywords:** Imaging, Mariana, LOKI, Doce River, Zooplankton.

## INTRODUCTION

The zooplankton assemblage comprises a diverse group of organisms that inhabit aquatic ecosystems around the world (SCHMID *et al.*, 2016). They play a key role in the organic matter transfer, from primary producers to higher trophic levels and, consequently, in the global carbon cycle (HIRCHE *et al.*, 2012). Copepods are the dominant group and thus constitute a fundamental link transferring energy along the marine food web and affecting the ecosystem dynamics (HARRIS *et al.*, 2000). As one of the most abundant organisms in the oceans, they frequently represent more than 90% of the marine zooplankton biomass (BRADFORD-GRIEVE *et al.*, 1999). They occupies a variety of niches as detritivores, herbivores, and carnivores consumers, but always depending on the prey size. This is the classical concept of the size-structured food web controlling the functioning of the environment. Understanding the spatial and temporal dynamics of organisms and how they interact with their environment is thus a crucial step in plankton ecology.

In plankton assemblage studies, the classical WP-2 cylindrical nets are the fundamental device used for zooplankton sampling (CALAZANS, 2011). This device integrates the whole plankton assemblage through depth and is inaccurate to address



spatial differences in the size distribution of copepods in the water column. Additionally, the time required to analyze many samples under microscopy imposes constraints on long-term studies or large geographical areas. For this reason, other tools have been improved, such as several environmental imaging systems, which provide fast and accurate *in situ* measurements of physical and biological properties of the ecosystem (BI *et al.*, 2015). In the last three decades, a great number of technologies capable of recording zooplankton images have been developed. This includes portable laboratory equipment, such as ZooScan, as well as *in situ* systems, such as 'Underwater Vision Profiler' (UVP), 'Zooplankton Visualization System' (ZOOVIS), 'Lightframe On-Site' (SOSPER), FlowCytobot, the Flow Cytometer and Microscope (FlowCAM), and the In Situ Ichthyoplankton Imaging System (ISIIS) (BLASCHKO *et al.*, 2005; SOSIK & OLSON, 2007; GROSJEAN *et al.*, 2004; GORSKY *et al.*, 2010; BI *et al.*, 2015).

Several instruments have been developed and used for automated particle analysis through the detection, counting and measurement of individual particles and planktonic organisms (CHRISTIAN *et al.*, 1998). The automatic methods, with their high acquisition potential, gather a great number of images, intensifying the analysis and treatment of images issues. The majority of these devices, however, are not suitable for acquisition of images of plankton in places of high turbidity. According to BI *et al.* (2015), the processing of images obtained from muddy waters, with high concentration of debris, remains a great challenge. Highly turbid waters reduce light penetration and add noise from light refraction and attenuation, preventing acquisition of high-quality images. This turbid condition difficulties the isolation, in a reliable way, of regions of interest (ROIs) that contain only single distinguishable objects at once, without losing any part of the target organisms. Hence, the number of particles in each image results in inaccurate estimation of ROIs and in numerous erroneously segmented objects. For instance, gelatinous plankton is particularly susceptible to fragmentation in multiple pseudo-organisms. This happens due to the uncertainty as to whether one marginal pixel actually belongs to the organism or to the background, as suspended solids in front of organisms represent a noise in the image.

An effective method to accurately identify and account for marine organisms, particularly copepods, would allow the reprocessing of samples stored in plankton collections, enabling new large-scale spatial and temporal projects to be carried out (HENZLER *et al.*, 2010). The development of copepod enumeration and classification algorithms would improve data analysis process and, therefore, would enable long-term environmental monitoring of the plankton dynamics. Considering the advantages of the

use of imaging systems as complimentary to the traditional techniques, this study aimed to develop a procedure to reduce noise in images obtained in waters with high quantity of suspended solids. On top of that, the main aims are to develop new algorithms that automatically enumerate and measure copepods *in situ*.

## METHODS

### Study site

To elaborate the processing algorithms, a set of images produced in two sites with different suspended sediment concentrations was selected. The images were obtained on November 27, 2015, a few days after the collapse of the dam located in Mariana (MG), when the waste with high suspended sediment load reached the outfall of the Doce River. During the operations of the R/V H39 "Vital de Oliveira", from the Brazilian Navy, images were recorded *in situ* through a Light Frame On-Sight Key Species Investigation (Isitech LOKI). The hauls were vertical from near the bottom with a mesh of 200  $\mu\text{m}$  and image acquisition rate of 20 frames per second (Figure 1). The hauls were carried out at two distinct points along the suspended solids concentration gradient. The first site (1) was located as closer as possible to the outfall of the Doce River, with expected high turbidity and shallow copepod assemblage (~20 meters deep). The second site (2) was located far from the Doce River opening with less turbid waters and deeper copepod assemblage (~100 meters).

The vertical profile of turbidity (NTU) and suspended particle concentration (CPS, particles  $\text{L}^{-1}$ ) in the two sites were simultaneously addressed using a turbidity sensor attached to a Multiparameter Datalogger (Horiba) and a Moving Vessel Profiler (MVP) equipped with a Laser Optical Plankton Counter (LOPC). The turbidity sensor was down from the deck up to 20 meters on both sites 1 and 2, and the water turbidity annotated. The MVP+LOPC was deployed from site 1 to site 2 with seven sequential launching.

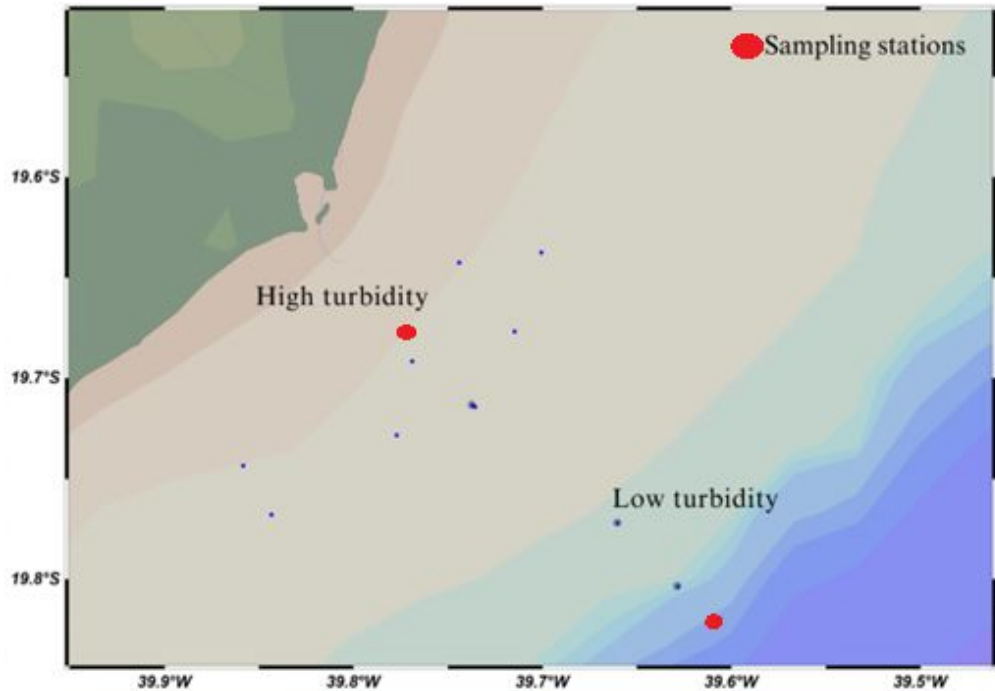


Figure 1. Map representing the collection points: one with high turbidity near the outfall, and the other with less turbidity farther away.

### The Light Frame On-sight Key Species Investigation (LOKI)

The LOKI is a system with 5 main parts: (1) A concentration net, with a mouth opening of 0.28 m<sup>2</sup> and a mesh aperture of 200 µm, (2) a computer with a solid state driver to store the images, (3) a CTD with temperature, pressure, dissolved oxygen, and fluorescence sensors, (4) a Prosilica GC 1380H (AVT-Allied Vision Technologies, Canada) with the Pentax 2514-M and (5) a battery. The full image size is 1360 × 1024 pixels, and the resolution is 23 µm per pixel, at 20 shots per second. It has a high-power LED unit, synchronized with the camera's exposure-shooting signal, which allows a fast shut-off time (55 µs) avoiding motion blurring that causes image distortion. In combination, it has an image channel 4 mm high (length = 31.3 mm, width = 20.75 mm, volume = 2.6 cm<sup>3</sup>), causing all the particles of the image to stay in focus. All images are stored in the LOKI solid state drive, where they can be accessed for further analysis. Once the recording starts instantly after power is on, a large amount of images are gathered either before or after the actual haul. From all images gathered since the equipment started functioning on ship deck, only those generated during the haul from near the bottom to the surface represent usable images of organisms in the water column and, therefore, are of interest for characterization and quantification of copepod populations. The distinction and separation of these images of interest were performed automatically by algorithms

elaborated in Python® (version 3.9) according to the actual depth measured by the pressure sensor. Hence, the onset of the haul was defined as the instant of maximum pressure (Figure 2). The end of the haul, in contrast, includes safety procedures to bring the LOKI back to ship deck. These procedures produce an oscillation in the equipment due to the waves at surface that is captured by the pressure sensors and might bias the density estimation near the surface (Figure 2). All images produced during this oscillation, therefore, were removed to avoid counting the same particle twice.

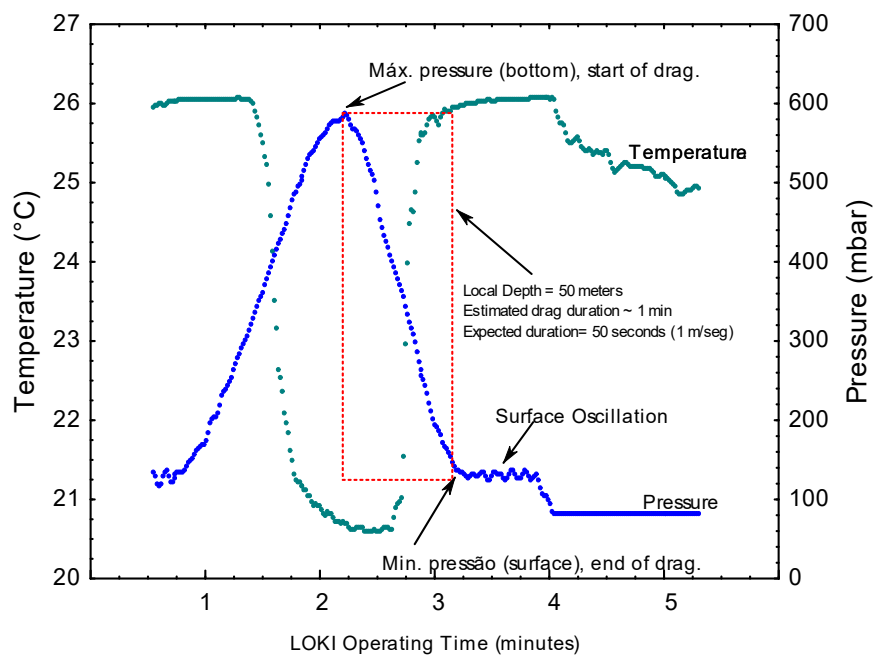


Figure 2. Example of vertical profile of temperature ( $^{\circ}\text{C}$ ) and pressure (mbar) during a LOKI haul. The red dotted square highlights the vertical haul from near the bottom back to the surface.

Once the images of the net ascent period were isolated from the full set, several smaller images (vignettes) were cut from the original full image and thus generated, each containing a prominent particle of the original image. To check if the counting and measurement steps are less accurate in places with high turbidity, thus biasing the estimation of copepod size and abundance, simultaneous manual and semi-automated procedures were compared. To perform the automated measurements of organisms surrounded by distinct amounts of suspended sediments, a subset of 1000 copepod vignettes were randomly selected and processed in 16 different binarization algorithms available in the ImageJ software (2.3.0). To maintain control over the test, the same set of

images was processed manually by an experienced taxonomist under visual inspection on the screen. The accuracy of each algorithm was calculated by the comparison of the morphometric measurements of the copepod's body (e.g., area, perimeter, and fitted ellipses) and counting made manually by the taxonomist and automatically by the ImageJ contour detection (function "*Analyze particle*", ImageJ).



Figure 3. Steps of the treatment of the images. A) Original vignette, automatically cropped by the LOKI system. B) Resulting binarization of vignette exemplified by the "Default" algorithm C) Resulting of the contour detection algorithm used in the copepod counting and measurement.

To improve the enumeration of copepods, three additional algorithms (algorithms 2 to 4) were elaborated with different sequential steps of treatment before the binarization (Table), bearing in mind that they followed the morphometry described above and the background processing. To evaluate the constancy and linearity of the results obtained in small samples (<1,000 images), the algorithms were tested again with 3 subsets of 100 random images from each site.

Algorithm 2 includes an increase in contrast before the binarization step to accentuate detail in the image, even though it may also accentuate 'noise' like suspended sediments (function '*Sharpen*' in ImageJ). This filter uses the following weighting factors to replace each pixel with a weighted average of the 3x3 neighbourhood:

$$\begin{array}{ccc} 1 & 1 & 1 \\ 1 & 2 & 1 \\ 1 & 1 & 1 \end{array}$$

The third algorithm used to estimate the abundance of copepods reduced the exposition of the vignettes to check if noise could be removed before the binarization step. The reduction of exposition was achieved by reducing each pixel value by 25 (function 'Math', ImageJ). Pixel values between 0 and 24 were set to zero. The fourth algorithm applies the 'Statistical Region Merging' algorithm (NOCK and NIELSEN 2004) to highlight the copepod from the surrounding suspended particles ('noise').

## RESULTS

### Images of interest

In total, 40375 vignettes were produced at the point with high turbidity (site 1) and 21664 at the point with low turbidity (site 2). Considering the different depths and operating times at each point, more vignettes were obtained in shallower highly-turbid waters (2018 vignettes m<sup>-1</sup>) than in deeper ones (217 vignettes m<sup>-1</sup>) (Table 1).

Table 1. Turbidity and particle concentration at the two sites.

	S	S
	ite 1	ite 2
Local Depth	2	1
	0 m	00 m
Turbidity (NTU) Surface	8	<
	.18	0.01
Turbidity (NTU) 20 meters	4	<
	12	0.01
Single Element Plankton (CPS, particles L <sup>-1</sup> )	>	<
	5000	1000
Total Vignettes	4	2
	0375	1664
Vignettes / m	2	2
	018	17

Each vertical haul last for nearly two minutes, starting approximately five minutes after the LOKI is powered on (Figure 4, red dotted rectangle). The operator procedures seem to have affected the performance of image acquisition. In site 1 (Figure 4A), the equipment was towed over nearly 20 meters (pressure ~ 260 mbar) for 2 minutes and a

half, with an oscillating minute in the surface (8'- 9'). In contrast, the net in site 2 was towed for 100 meters (5x longer) for only 2 minutes, with no oscillation near the surface.

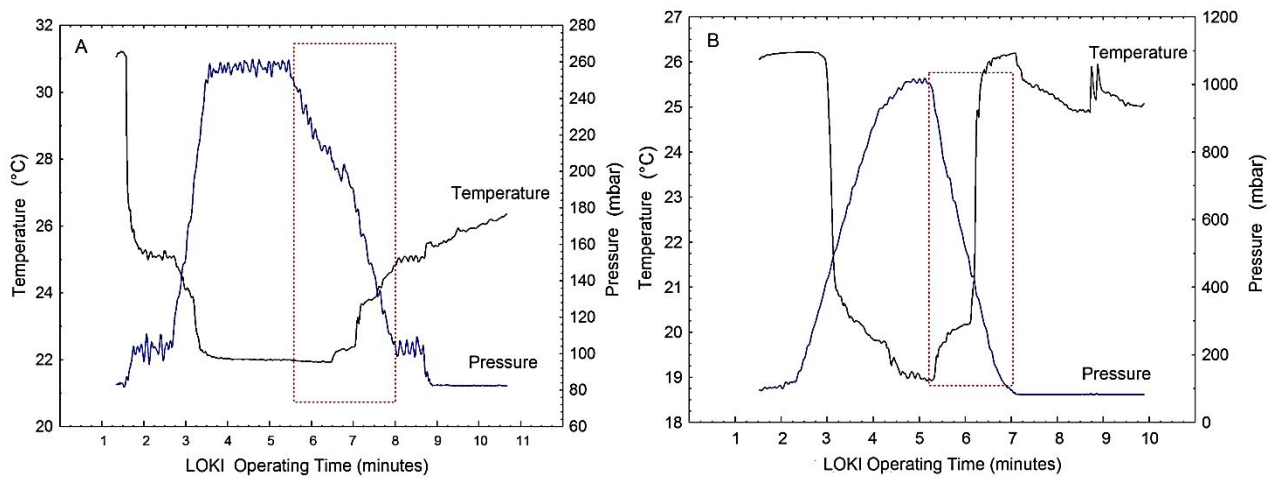


Figure 4. Vertical profiles of temperature ( $^{\circ}\text{C}$ ) and pressure (mbar) during the two LOKI hauls at the point with high turbidity (A, site 1) and low turbidity (B, site 2). The red dotted rectangles highlight the accepted vertical haul from which images were analyzed

The water turbidity was different between sites. The number of particles in suspension near site 1 was one-fold higher than that at site 2 (Figure 5), particularly near the bottom.

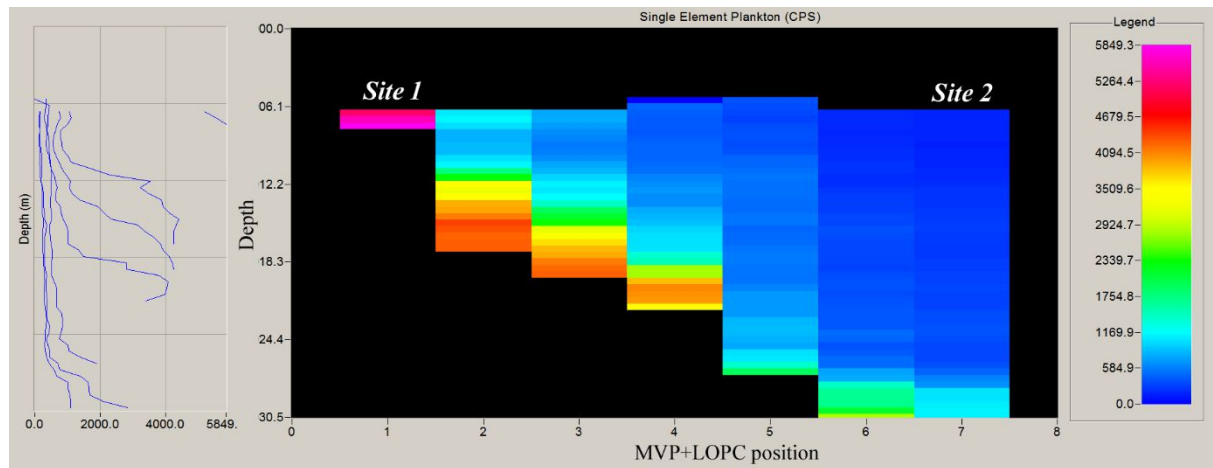


Figure 5. Laser-Optical Plankton Counter (LOPC) profile from site 1 (position 1) to site 2 (position 7) after seven sequential deployments showing the gradient of suspended particles. The scale of particle counts (Single Element Plankton) is on the right.

### Image cropping

The performance of the LOKI system in automatic crop vignettes was affected by the turbidity and concentration of suspended particles (Table 2). From 1000 randomly selected images obtained under high turbid waters (site 1), the majority (96%) were badly or non-segmented full images that need additional processing steps. In contrast, under

less turbid waters (site 2), nearly 99% of the stored images were correctly segmented vignettes.

Table 2. Comparison of the performance of LOKI segmentation algorithm in cropping vignettes under high and low turbidity.

Automatic Crop	High Turbidity	Low Turbidity
<b>Vignettes (well-segmented full organism)</b>	20	986
<b>Badly segmented vignettes or non-segmented images</b>	960	14

Small particles dominated in site 1 with higher turbidity as revealed by the predominance (>60%) of files between 1 and 10 kb in the set of vignettes (Figure 6A), while those from site 2 predominate in the 10-50 kb. Full images resulting from failed segmentation have 1.2 Mb and were more frequent under high turbidity.

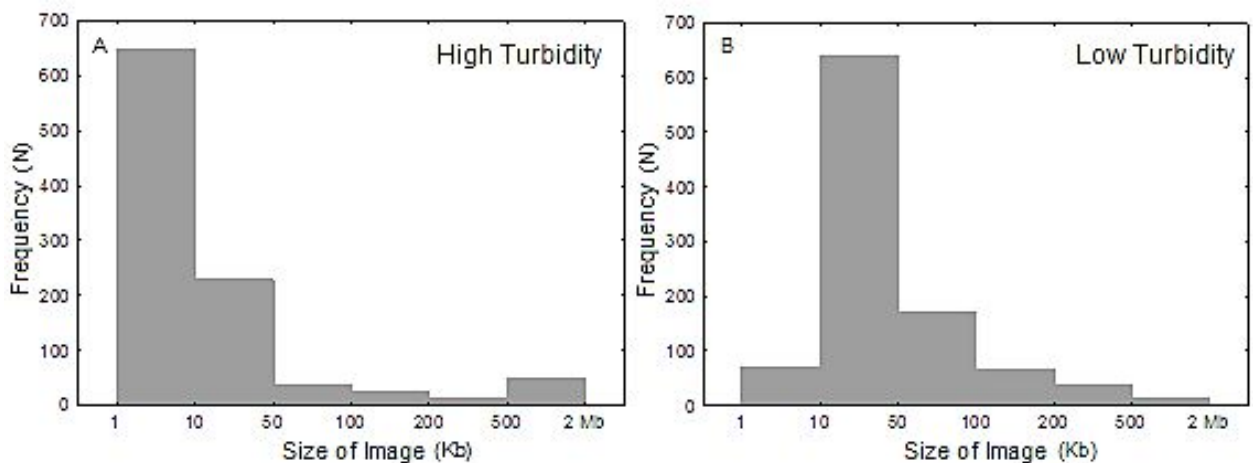


Figure 6. Distribution of size classes of the files, on the “x” axis, the size of the particles in kilobytes, and on the “y” axis, the frequency of the particles. In the histogram as the image “a” point with high turbidity, and in “b” point with low turbidity.

The presence of suspended sediments can be seen in vignettes from site 1 as white dots around the copepods (Figure 7A). In contrast, copepods from site 2 with less suspended sediments have less ‘noise’ and the resulting histogram of grayscale values is less skewed to the right (Figure 7B). Nevertheless, the presence of ‘noise’ in the vignette was not detected in the derived statistics as exemplified in Figure 7. Both pictures have very similar mean, for example (Table 3), although the vignette with higher contrast exhibits a slightly higher mode meaning more dark pixels (Figure 7B).



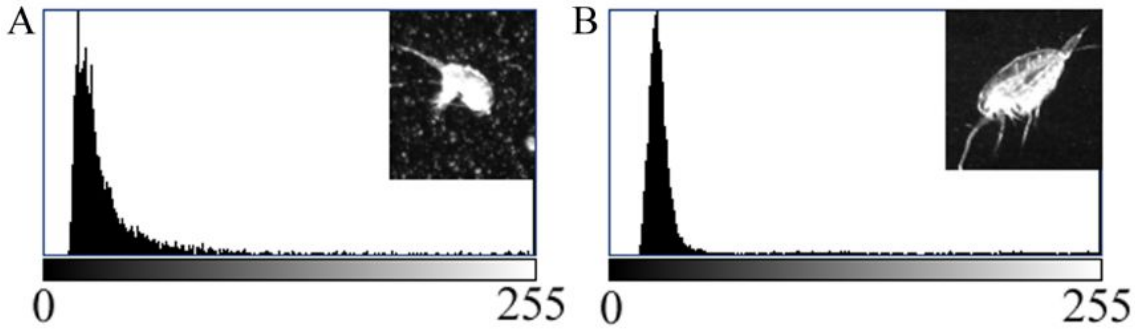


Figure 7. Examples of in situ photography (grayscale) and the corresponding histogram showing more suspended sediments ('noise') around the copepod in site 1 (A) than in the copepod in site 2 (B).

Table 3. Statistics of the above grayscale images (vignettes) from site 1 (with high 'noise') and site 2 (with low 'noise').

	High 'noise'	Low 'noise'
Number of Pixels	6688	22496
Mean pixel value (grayscale)	50	56
Standard Deviation	60	68
Minimum	12	13
Maximum	255	255
Mode	17	24
# pixels in the Mode	376 (5.62%)	1633 (7.26%)

### Binarization performance in discriminating one single copepod

Our result suggested that a stronger binarization algorithm eroding the copepod's body leads to better estimates of copepod abundance. Most binarization algorithms eroded the thinnest parts of the body, like the first antennae, and thus resulted in multiple fragments counted independently as one entire organism. Thus the choice of the least impactful algorithm for automatic 'noise' reduction in the copepod body (Figure 8) resulted in more fragments and less accurate counting (Figure 9). Our results suggested that the minimum point between the two medians, automatically set by the 'Minimum' algorithm, almost exclusively contrasted the copepod prosome (Figure 8I).

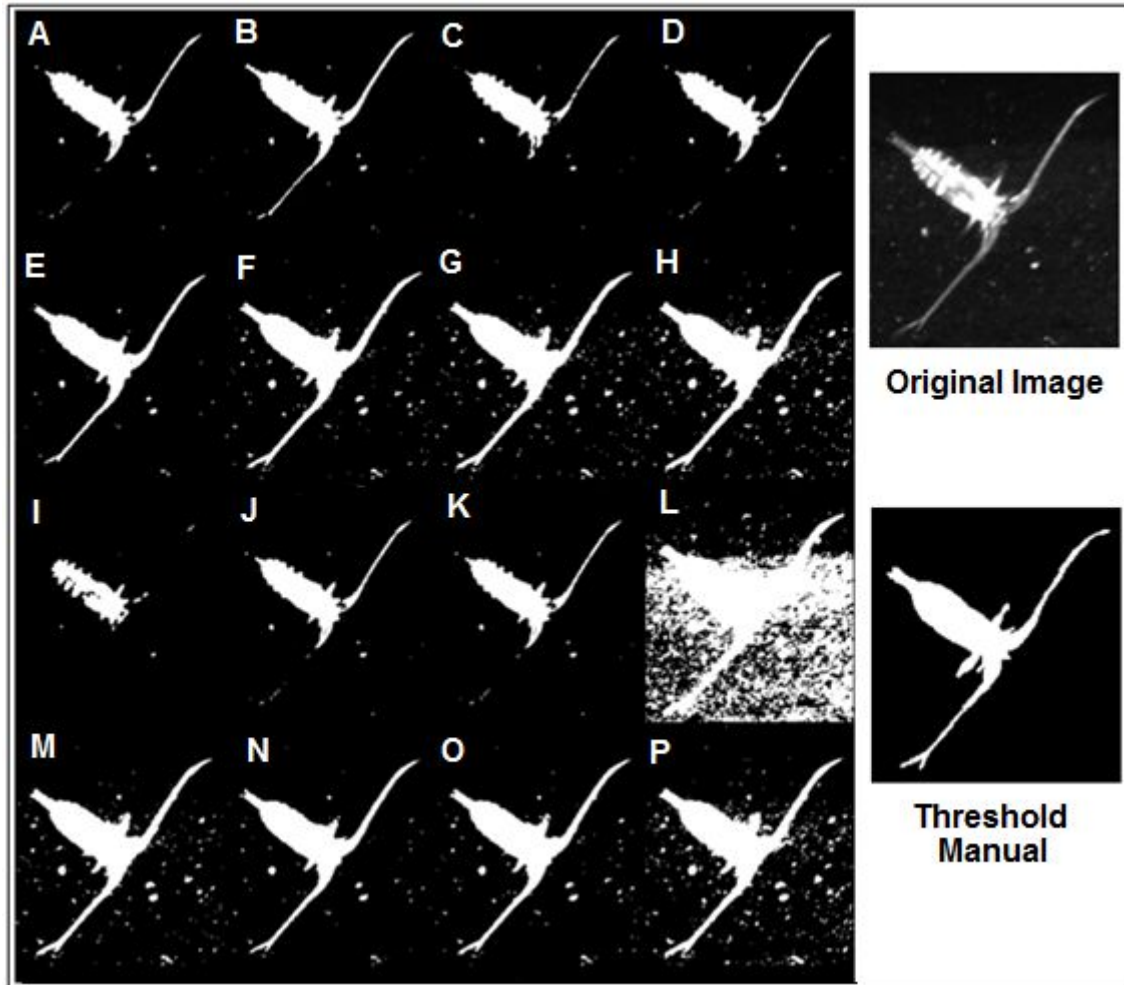


Figure 8. Performance of the 16 binarization methods (A-Default, B-Huang, C-Intermodes, D-IsoData, E-Li, F-MaxEntropy, G-Mean, H-MinError, I-Minimum, J-Moments, K -Osu, L-Percentile, M-RenyiEntropy, N-Shanbhag, O-Triangle, P-Yen) available on ImageJ, compared to the manual method.

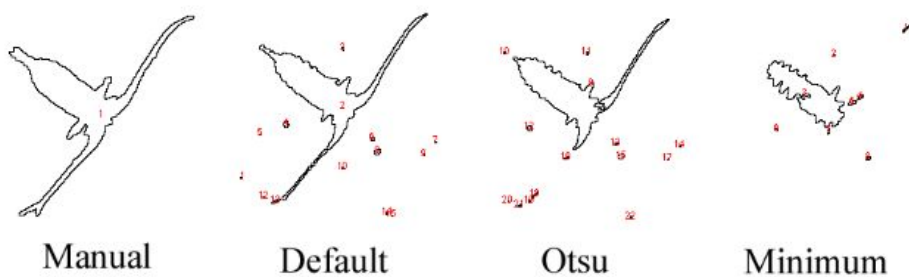


Figure 9. Fragmentation of copepod's body after binarization by 'default', 'Otsu', and 'Minimum' algorithms, compared to the actual copepod contour (manual). The number of fragments is signaled in red.

### Size of the copepod

The average area of a copepod body (prosoma + urosome) was 312639  $\mu\text{m}^2$  (= 591 pixels<sup>2</sup>). The high standard deviation (369 pixels<sup>2</sup>) suggested wide variation in the size. Several automatic algorithms resulted in a high linear correlation ( $R^2 > 80\%$ ) with the actual copepod's size (Figure 10). Differently from counting, the 'Minimum' algorithm excessively eroded the body (Figure 9) and lead to strong errors in measuring the organisms. The 'Renyi Entropy' algorithm resulted in the highest correlation ( $R^2 = 0.895$ , Figure 10M).

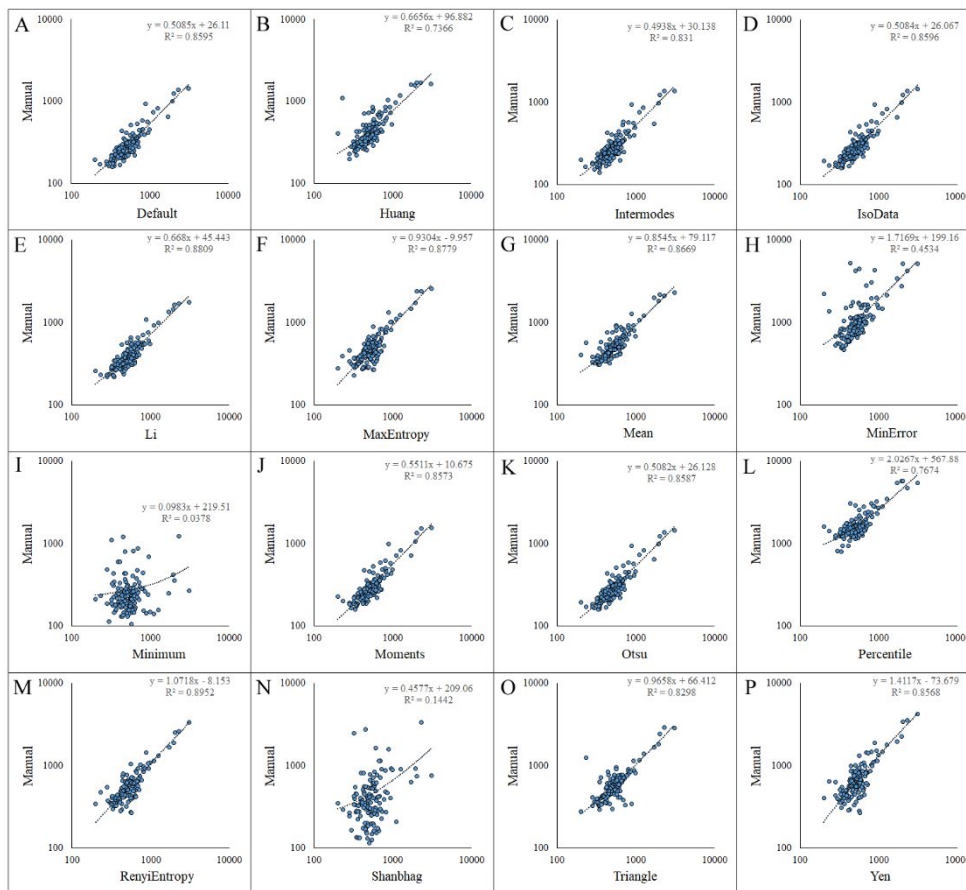


Figure 10. Relationship between the copepod's body area as estimated from 16 automatic algorithms and the actual area manually measured. The linear regression equation and the  $R^2$  for each algorithm are shown inside the scatterplot.

## Enumeration algorithm

The copepod count test based on the four developed algorithms revealed percentages of accuracy between 90% and 507% (Table 4). The resulting counting was overestimated in turbid waters when images have increased contrast (507%) or are treated with the SRM algorithm (357%). The most efficient method for either turbid or clear water is binarization without additional pre-treatment, although under high turbidity the

counting was less efficient, reaching up to 95% (644 organisms) of the total copepods (678 organisms) present. Under low turbidity, the binarization ended with more organisms (113%) than the actual counting (1038 copepods).

Table 4. Comparison of the number of copepods estimated visually by an expert (visual inspection, 100%) and automatically following four algorithms elaborated in ImageJ.

	<b>Copepod Count</b>			
	High Turbidity		Low Turbidity	
<b>Visual inspection</b>	678	100%	1038	100%
<b>Algorithm 1: Only Binarization</b>	644	95%	1176	113%
<b>Algorithm 2: Increased contrast + Binarization</b>	3441	507%	1782	171%
<b>Algorithm 3: Reduced exposition- + Binarization</b>	612	90%	1178	113%
<b>Algorithm 4: Statistical Region Merging + Binarization</b>	2423	357%	1937	186%

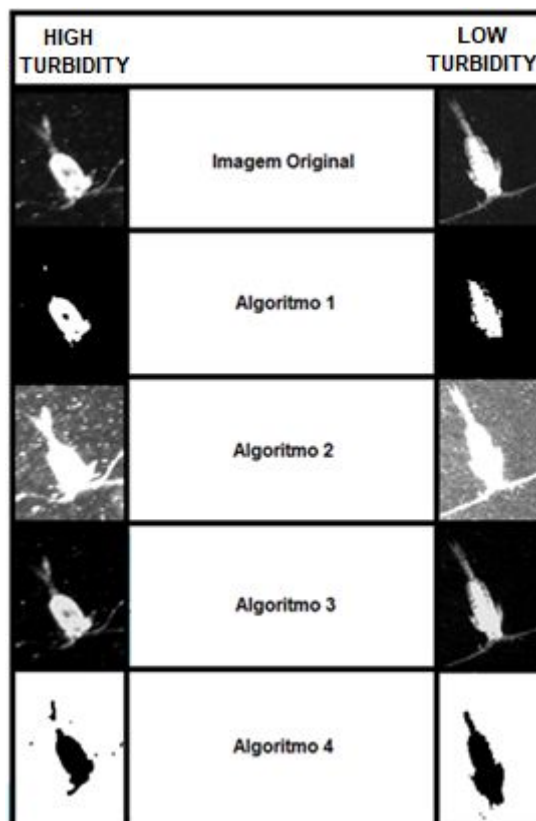


Figure 11. Comparison between two points with different turbidity conditions in the treatment using the four algorithms.

## DISCUSSION

Considering the factors of operation time, local depth and turbidity, the results point to water turbidity as the most effective factor in the generation of multiple ROIs. A similar result was observed in the study by (BI *et al.* 2015), who pointed out the advantages of plankton image treatment methods designed for controlling conditions of less turbid water to result in more consistent and high-quality images. The speed of a vertical haul, although subjected to sea conditions and the winch, should be kept as close as possible to 1 meter per second (BOLTOVSKOY, 1981).

The images used for the accomplishment of this research were acquired in a place with high turbidity, provoked by the contribution of muddy sediments, which scattered the light in the image, hindering the software while it tried to decide on segmenting a potential organism or not. In (BI *et al.* 2015) study, it was emphasized that the processing of images obtained from turbid waters remains a great challenge. First, high turbidity water attenuates and scatters light more quickly than clear ones, reducing visibility and limiting the performance of the equipment in acquiring high-quality images. One of the main problems in identifying the images was the number of particles in the background. (ÁLVAREZ *et al.* 2012) have pointed out that the presence of debris in the samples is, however, a common feature of plankton imaging devices.

SCHULZ *et al.* (2010) highlighted problems in the gathering of zooplankton images with camera systems, among them the low image quality used for taxonomic identification. The presence of scattered material that is not the target object in the water increases the difficulty in distinguishing the particles of interest (BI *et al.*, 2015). The objects within each image were separated from the background by a process called segmentation. (SUROVY *et al.* 2014) described the difficulty found in the segmentation of vegetable images, with low contrast, being able to have the vegetable roots fragmented and the measurement and counting underestimated.

Segmentation is a vital part of image processing (NATCHIMUTHU *et al.*, 2013). In this research, it was possible to observe segmentation problems on the images from points with high turbidity, in the pre-treatment stage. At these points, the segmentation of a single copepod in the middle of suspended solids by the LOKI program was partially successful. Elaborating an algorithm that separates the object of interest from the background simplified the tests with algorithms for enumeration of organisms by the size of their area, and that was paramount for the accomplishment of this study.

However, (CASTRO *et al.* 2007) and (ESCRIBANO *et al.* 2009) carried out detailed analysis of the vertical distribution of organisms, using LOKI, without segmentation

problems. According to (SIERACKI *et al.* 2007), imaging systems can record the distribution of plankton on a fine scale. Nevertheless, the flaws pointed out in this research indicate the need for additional algorithms to improve current systems, regarding the enumeration and classification of copepods in high turbidity environments.

In choosing the threshold method, the integrity of the organism's body was fundamental after cleaning the background. (SCHMID *et al.* 2016) have pointed out that in traditional copepod taxonomy, the length of the prosome is often used to identify species rather than the total length. The Otsu method is described by (SAHOO *et al.* 1988) as a global threshold method for the separation of particles or background objects and is also described in the studies of (PING-SUNG *et al.* 2001) and (HONGMIN *et al.* 2014). Nevertheless, (SUROVY *et al.* 2014) concluded that the degree of precision in the estimation of the size of an analyzed object's area – particularly in the images of plant structure –, is due to the correct selection of the threshold. According to (BI *et al.* 2015), it is difficult to use a single global threshold value to convert grayscale images to binary images. Due to uneven lighting over the visual field, it is difficult to impose a threshold above, in which all pixels become white, and below, in which they become black. Our results suggested that studies aiming at copepod counting and measurement need specific thresholds.

NATCHIMUTHU *et al.* (2013) found 97% accuracy in their automatic enumeration and classification of microalgae by size and shape. During this research, the four algorithms that were elaborated to count and measure copepods resulted in highly distinct counting. It was found in one of the algorithms a similarity of 96% with the manual method. (SCHMID *et al.* 2016) obtained in their study a loss of the smaller and more translucent copepods, probably due to the algorithm that detects the particle when passing through the camera flow.

The number of organisms counted as copepods by most semi-automated procedures tends to be smaller than the manual counts (~ 10 fewer) (BI *et al.*, 2014). Our results, in contrast, revealed that counting could be either under or overestimated. We hypothesized that multiple 'chimaera particles' would arise depending on the contour detection step. The presence of chitin in the exoskeleton of copepods usually culminates in a well-identifiable body contour, but the appendages and antennae are generally not clear enough, probably due to the small size or the camera shutter speed (SCHULZ *et al.*, 2010). FOREST *et al.* (2012) found a striking difference between the estimated biovolume in the ZooScan analyses and the morphometric estimates of manual counts. SCHULZ *et al.*

(2010) found about 15% of debris and undesirable particles in their particle count results. The measurements performed in this study, in contrast, were highly similar to the actual copepod size and are good estimates of populational size classes.

Automated and semi-automated zooplankton imaging systems have long been sought as part of a modern approach to monitoring the marine environment. The need for sensors capable of providing abundance and biomass data in high resolution over an extent of time has generated a growing effort to bridge the gap between different contemporary sampling methods in marine sciences (BASEDOW *et al.*, 2013). The results acquired in this research highlighted the future trend in the improvement of the available plankton image processing technologies, particularly regarding better algorithms for counting and measurement.

### **ACKNOWLEDGEMENTS**

We are grateful to the IEAPM/Brazilian Navy and all those who have worked on the sampling and analysis.

### **FUNDING**

Financial support to the development of this study was provided by the CNPq (Proc. 441525/2016-4)

### **REFERENCES**

ÁLVAREZ, E., López-Ururutia, Á., & Nogueira, E. (2012). Improvement of plankton biovolume estimates derived from image-based automatic sampling devices: Application to FlowCAM. **Journal of Plankton Research**, 34(6), 454-469. <https://doi.org/10.1093/plankt/fbs017>

BACHILLER, E., Fernandes, J.A., (2011). Zooplankton Image Analysis Manual: Automated identification by means of scanner and digital camera as imaging devices. 18(2): 16-37. **Revista de Investigación Marina**.

Basedow, S. L., Tande, K. S., Norrbin, M. F., & Kristiansen, S. (2013). Capturing quantitative zooplankton information in the sea: Performance test of laser optical plankton counter and video plankton recorder in *Calanus finmarchicus* dominated summer situation. **Progress in Oceanography**. 108(April 2016), 72-80. <https://doi.org/10.1016/j.pocean..2012.10.005>

Benfield, M.C., Grosjean, P., Culverhouse, P.F., Irigoien, X., Sieracki, M.E., Lopez-Urrutia, A., Dam, H.G., Hu, Q., Davis, C.S. & Hansen, A. (2007). RAPID: research on automated plankton identification. ***Oceanography***, 20: 172-187

Bi, H., Guo, Z., Benfield, M. C., Fan, C., Ford, M., Shahrestani, S., & Sieracki, J. M., (2015). A semi-automated image analysis procedure for in Situ plankton imaging systems. **PLoS ONE**, 10(5), 1-17. <https://doi.org/10.1371/journal.pone.0127121>

Blaschko, M. B., Holness, G., Mattar, M. A. *et al.* (2005) Automatic in situ identification of plankton. Proceedings of the Seventh IEEE Workshops on Application of Computer Vision (**WACV/MOTION'05**), 1, 79–86.

Bradford-Grieve, J. M.; Markhaseva, E.I.; Rocha, C. E. F., (1999). Copepoda. In: Boltovskoy, D. (Ed.). South Atlantic Zooplankton. Leiden. Backhuys Publishers, V. 2, p. 869-1098.

Calazans D., Muelbert J. H., e Muxagata E. (2011). **Estudos Oceanográficos:do instrumental ao prático**. capítulo 9. página 200-274.

Castro, L.R., Troncoso, V.A., Figueroa, D.R., (2007). Fine-scale vertical distribution of coastal copepods in the Golfo de Arauco, central Chile, during the upwelling season. **Prog. Oceanogr.** 75, 486-500.

Davis, C. S., Hu, Q., Gallager, S. M. *et al.* (2004) Real-time observation of taxa-specific plankton distributions: an optical sampling method. **Mar. Ecol. Prog. Ser.**, 284, 77–96.

Dietrich A. and Uhlig G., Crustaceana. Supplement No. 7, Studies on Copepoda II (Proceedings of the first International Conference on copepoda, Amsterdam, the Netherlands, 24-28 August 1981) (1984), pp. 159-165. Published by: Brill, Stable URL: <http://www.jstor.org/stable/25027550>

Forest A., Stemmann L., Picheral M., Burdof L., Robert D., Fortier L., Babin M. (2012). Size distribution of particles and zooplankton across the shelf-basin system in southeast Beaufort Sea: combined results from an Underwater Vision Profiler and vertical net tows. **Biogeosciences**, 9, 1301-1320.



Frontier, S. Atlas del Zooplancton del Atlántico Sudoccidental y métodos de trabajo con el zooplancton marino. Mar del Pçata: **INIDEP**, (1981).

Gonzalez, R. C., Woods R. E., and Eddins S. L. (2004). Digital Image Processing Using MATLAB. Prentice Hall. pag. 72.

Gorsky, G., Ohman, M. D., Picheral, M. *et al.* (2010) Digital zooplankton image analysis using the ZooScan integrated system. **J. Plankton Res.**, 32, 285–303.

Grosjean, P., Picheral, M., Warembourg, C. *et al.* (2004) Enumeration, measurement and identification of net zooplankton samples using the ZOOSCAN digital imaging system. **ICES J. Mar. Sci.**, 61, 518–525.

Henzler, C.M., Hoaglund E.A., Gaines S. D., (2010). FISH-CS – a rapid method for counting and sorting species of marine zooplankton. **Marine Ecology Progress Series**, 410, 1-11. Retrieved from <http://www.jstor.org/stable/24873996>

Hirche, H. J., Schulz, J., & Hanken, T. (2012). A modular imaging system for collection and analysis of live and preserved zooplankton samples. Program Book – OCEANS 2012 MTS/IEEE Yeosu: The Living Ocean Coast – **Diversity of Resources and Sustainable Activities**.<https://doi.org/10.1109/OCEANS-Yeosu.2012.6263514>

Hongmin C., Zhong Y., Xinhua C., Weiming X., Xiaoyin X. (2014). A New Iterative Triclass Thresholding Technique in Image Segmentation. **IEE TRANSACTION ON IMAGE PROCESSING**, Vol. 23, NO. 3. <http://redpel.com+917620593389>

Hu Q., e Davis C., (2005). Automatic plankton image recognition with co-occurrence matrices and Support Vector Machine. **Marine Ecology Progress Series**. June 23, vol. 295:21-31,2005. Inter Research. <http://www.int-res.com>

Luo, T., Kramer, K., Goldgof, D. B. *et al.* (2004) Recognizing plankton images from the shadow image particle profiling evaluation recorder. **IEEE Trans. Syst. Man Cyber. B**, 34, 1753–1762.

Natchimuthu S., Chinnaraj P., Parthasarathy S., Senthil K., (2013). Automatic Identification of Algal Community from Microscopic Images. *Bioinformatis and Biology Insights*. Volume 7. October 10, 2013. <http://doi.org/10.4137/BBI.S12844>

Ping-Sung L., Tse-Sheng C., Pau-Choo C. (2001). A Fast Algorithm for Multilevel Thresholding. *Journal of Information Science and Engineering*. 713-727 pag. December 30. [http://www.iis.sinica.edu.tw/JISE/2001/200109\\_01](http://www.iis.sinica.edu.tw/JISE/2001/200109_01)

Sahoo, P.K., Soltani, S., Wong, A.K., Chan, Y.C., (1988). A survey of threshold techniques. *Computer Vision, Graphics and Image Processing* 41, 233-260.

Schmid, M. S., Aubry, C., Grigor, J., Fortier, L. (2016). The LOKI underwater imaging system and an automatic identification model for the detection of zooplankton taxa in the Arctic Ocean. *Methods in Oceanography*. DOI: 10.1016/j.mio.2016.03.003

Schulz, J., Barz, K., Ayon, P., Ludtke, A., Zielinski, O., Menedoht, D., Hirche, H. J., (2010). Imaging of plankton specimens with the lightframe on-sight keystone investigation (LOKI) system. **Journal of the European Optical Society – Rapid Publications** 5, 10017s.

Sosik, H. M. and Olson, R. J. (2007) Automated taxonomic classification of phytoplankton sampled with imaging-in-flow cytometry. **Limnol. Oceanogr. Meth**, 5, 204–216.

Sieracki M. E. *et al* (2007)., Research on Automated Plankton Identification. **Oceanography**. Vol. 20, N° 2. Published June 2007. DOI: 10.5670/oceanog.2007.63 · Source: OAI

Surovy P., Dinis C., Marusak R., Ribeiro N. de A., (2014). Importance of automatic threshold for image segmentation for accurate measurement of fine roots of woody plants. **Lesnícky Casopis Forestry Journal**. 60 244-249. <http://www.nlcsk.sk/fj/>

Tang, X., Stewart, W. K., Vincent, L. *et al*. (1998) Automatic plankton image recognition. **Artif. Intell. Rev.**, 12, 177–199.

Wiebe, P.H. & Benfield, M.C. (2003). From the Hensen net toward four-dimensional biological oceanography. **Progress in Oceanography**, 56:7-136

Zarauz, L., Irigoien, X. and Fernandes, J. A. (2009) Changes in plankton size structure and composition, during the generation of a phytoplankton bloom, in the central Cantabrian Sea. **J. Plankton Res.**, 31, 193–207.

**CAPÍTULO II:****NEW DIVERSITY INDEX TO ESTIMATE THE PLANKTONIC ASSEMBLAGE WITH IMAGES ON THE ECOTAXA WEBSITE**

Thiago da Silva Matos<sup>1</sup>, Carolina Siqueira dos Reis<sup>1</sup>, Laura de Andrade Moura<sup>2</sup>, Ricardo Coutinho<sup>1,2</sup>, Lohengrin Fernandes<sup>1,2</sup>

T.M.: [ORCID® 0000-0002-9390-7669](#)

C.R.: [ORCID® 0000-0003-1584-0988](#)

M.A.: [ORCID® 0009-0006-0633-9429](#)

L.M.: [ORCID® 0000-0003-0002-9981](#)

R.C.: [ORCID® 0000-0001-5430-2176](#)

L.F.: [ORCID® 0000-0002-8579-2363](#)

<sup>1</sup>IEAPM/UFF Marine Biotechnology Post-Graduate Program.

<sup>2</sup>Instituto de Estudos do Mar Almirante Paulo Moreira.

(Instituto de Estudos do Mar Almirante Paulo Moreira, Departamento de Biotecnologia Marinha, Divisão de Biotecnologia Aplicada. Rua Kioto, 253; Praia dos Anjos; 28930-000 - Arraial do Cabo, RJ – Brasil).

**TSM** e-mail: [biologo.thiagomatos@gmail.com](mailto:biologo.thiagomatos@gmail.com)

**CSR** e-mail: [carolinasreis@gmail.com](mailto:carolinasreis@gmail.com)

**LAM** e-mail: [laura\\_moura@outlook.com](mailto:laura_moura@outlook.com)

**MA** e-mail: [marcio-abreu@hotmail.com](mailto:marcio-abreu@hotmail.com)

**RC** e-mail: [rcoutinhosa@yahoo.com](mailto:rcoutinhosa@yahoo.com)

**LDAF** e-mail: [lohengrin.fernandes@gmail.com](mailto:lohengrin.fernandes@gmail.com)

**\*CORRESPONDING AUTHOR**

Thiago da Silva Matos

[biologo.thiagomatos@gmail.com](mailto:biologo.thiagomatos@gmail.com)

**ABSTRACT**

One of the most important biological components to understand and assess ecosystem status is the planktonic assemblage, through its abundance, biomass and diversity. Among the indices to estimate beta diversity, the Shannon index is the most

used since its introduction in the 366 this activity demands a lot of effort and time spent with the analyzes. In recent years, several plankton image acquisition devices have been developed to optimize results and enable the understanding of ecosystems and their processes, including machine learning algorithms and artificial intelligence, as used by the ECOTAXA website to perform the classification of each image. (body). However, given the advances in these image classification algorithms, estimating plankton diversity through these tools is still a challenge, as there is no index developed for such activity. This work developed based on the mathematics of the Shannon diversity index, a new diversity index to work with the images on the ECOTAXA website, the Image Diversity Index (IDI). This new diversity index was used to estimate holoplankton diversity in a time series in the Cabo Frio Resurgence region in Arraial do Cabo. The diversity of classes was correlated with the temperature and salinity parameters of the water, both at the bottom and on the surface. The results showed a variation in image class diversity over time, between 0.38 and 2.04 ( $\pm 0.28SD$ ) bits.class<sup>-1</sup>. An annual increase in temperature was also observed, accompanied by an increase in diversity.

**Keywords:** Plankton, Image Diversity Index, ECOTAXA, Imaging, Data base.

## INTRODUCTION

The name plankton means “wandering” according to its Greek origin, it is composed of an organism with insufficient displacement power to break the dynamics of water masses and currents in the aquatic environment (BONECKER *et al.*, 2008), these organisms are transported passively or in water movements (BOLTOVSKOY, 1981). The planktonic assemblage is composed of organisms smaller than 2  $\mu\text{m}$  up to 2000  $\mu\text{m}$ , classified as: picoplankton < 2  $\mu\text{m}$ , nanoplankton 2-20  $\mu\text{m}$ , microplankton 20 – 200  $\mu\text{m}$ , macroplâncton 200 – < 2000  $\mu\text{m}$  (SIEBURTH *et al.*, 1978; BEARDALL *et al.*, 2009). These organisms are fundamental for the maintenance of life on planet Earth, especially with photosynthetic organisms, responsible for Half of global primary production (BEHRNFELD *et al.* 2001).

Zooplankton specifically have a key position in food webs once they are the primary predators, acting as a bridge between planktonic primary producers (phytoplankton) and the upper trophic levels (RICHARDON, 2008). The knowledge of the distribution and

diversity of these organisms helps to understand the status of the marine ecosystem and its dynamics, enabling environmental preservation actions (BORJA *et al.*, 2013; TETT *et al.*, 2013). Hence, there is a continuous effort to develop tools and processes for automatic counting and classification of plankton. Several image acquisition instruments have been developed in recent decades, but the counting and classification systems performed by algorithms with maximum accuracy is still a challenge.

Plankton heterogeneity is usually estimated by traditional methods, such as alpha diversity indices (Margalef), dominance indices (Simpson), and indices of probability of occurrence (Shannon) (MAGURRAN, 2004). However, these indices, formulated in the 1960s, have been little improved until now, so that newer techniques such as flow cytometry and metagenomics eventually develop their own protocols for diversity analysis (ATAKY, 2022). Diversity - or Biodiversity - is a biological parameter that tries to estimate the variability of life forms, usually species, in an ecosystem. There are many useful estimates of variety among biological entities, each following specific goals and targets. Taxonomic, genetic, and functional diversities are the most common approaches to biodiversity, although there are also more modern ones such as texture diversity (ATAKY, 2022).

In general, these diversity indices consider three basic assumptions, namely that (i) all 'species' - or entities - are included and treated equally, with no distinction between rare and dominant, (ii) all individuals are included and treated equally, regardless of size, and (iii) species abundance is recorded using appropriate and comparable units (MAGURRAN, 2004). In addition to the error associated with the skill of the taxonomist and the selectivity of the plankton net mesh, species are likely to be considered as a species group or another super specific taxon after taxonomic review. Therefore, ecological diversity tends to be underestimated or subjective, and broad approaches may shed some light on diversity estimation (GOTELLI and COLWELL, 2001).

In addition to plankton heterogeneity as estimated by diversity, the spatial and temporal dynamics of key populations are also often assessed from the perspective of variations in population abundance (density) and average individual size. Thus, planktonic communities may be more or less diverse, populations may be more or less numerous, and individuals may be larger or smaller over time. These three sources of oscillation are the target of the current chapter.

## MATERIAL AND METHODS

### Study Site

Plankton samples were collected in a fixed station in Cabo Frio Island (23°S - 042.01°W), as part of the Long-term Ecological Research (LTER) “Upwelling” Project (PELD-RECA), by sub-superficial horizontal hauls lasting for 3 minutes with a cylindrical-conical net, 40 cm mouth opening, 100 µm mesh size, and equipped with a calibrated flowmeter (Model 2030R Mechanical Flowmeter, General Oceanics Inc., Miami, FL) to estimate the water volume that was filtrated.

Immediately after collection, samples were split at the laboratory with a Folsom Plankton Splitter (BOLTOVSKOY, 1981). One sub-sample was submitted to manual counting using microscopy and the other was submitted to image acquisition using a Benchtop B3 FlowCAM cytometer (FlowCAM®, Fluid Imaging Technologies, Yarmouth, ME, EUA) configured in auto imaging mode with 2x objective and 2000µm x 200µm flow cell (width x depth). Images were captured at 2400 dpi resolution, with a size of 1024 x 768 pixels, 17 frames per second and a flow rate of 10 ml/min. A magnetic stirrer was used to keep the particles in suspension and the sample concentration homogeneous during the analysis. Sample run interruptions were set on 4,000 particles in total. Visual Spreadsheet Software (VSP), version 3.4.5 (FLUIMAGING TECHNOLOGIES, 2013), was used for prior analysis and measurement of organisms.

After the run, the images were pre-treated to split each Region of Interest by using coupled Python and ImageJ software (‘Analyze Particles’ function). The images were treated using a Python software routine to merge metadata to the image and an ImageJ routine for background cleaning, removing noise and preserving the main particle (algorithms and tools). After this treatment, the images were uploaded to the EcoTaxa platform (<https://ecotaxa.obs-vlfr.fr/prj/6015>) where, after the automatic prediction and validation of the vignettes, the classification of the organisms was performed (PICHERAL *et al.*, 2017).

The abundance and the taxonomic composition of the organisms were analyzed (SIERACKI *et al.*, 1998). For statistical analysis, the data were processed with R software (R CORE TEAM, 2008)

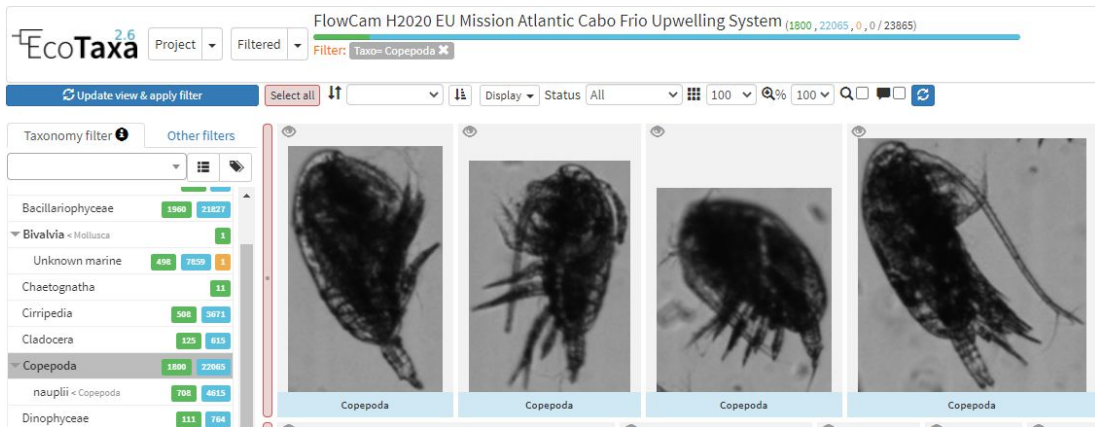


Figure 12. EcoTaxa website interface (<https://ecotaxa.obs-vlfr.fr/>). The researcher can browse the database along a taxonomic tree (as in the example on the left of the image) or filter the images according to sampling criteria (location, time, depth) or even morphological characteristics such as (size, chlorophyll a, among others). Fast identification of a large set of images is performed by combining machine learning and human validation.

The new diversity index applied to the ECOTAXA images has similar mathematics to the Shannon index, but instead of using the number of species, it uses the number of vignettes in the ECOTAXA. As it is not possible to always establish by species, varying between family, genus and species, the unit used was the OTU - Operational Taxonomic Unit.

For diversity estimation, the new IDI (Image Diversity Index).

$$IDI'c = -\sum_{(i=1)}^S \left[ \pi_i \ln \pi_i \right]$$

where,

S = number of image classes (43),

$\pi_i$  = proportion of vignettes belonging to class i to the total number of vignettes (277,481).

## RESULTS

To estimate plankton heterogeneity and proportionality as a potential proxy of diversity, 6,069,222 photomicrographs (vignettes) of organisms and tryptonic particles obtained in FlowCAM were classified into 108 functional categories. Forty-three categories were selected (Table 5) that total 277,481 photomicrographs (vignettes) and represent at least one organism, regardless of its life stage, and excluded the classes of particles and other forms of trypton. The category name refers to the likely dominant organism in the group, without implying that there is only a single species. The taxonomic resolution in use does not allow us to conclude on the number of taxa in each category. However, the classification algorithm remained constant for all samples and all vignettes, thus



maintaining the internal consistency of the data generated. Thus, the criteria for machine learning and organism classification were the same throughout the study.

For diversity estimation, the new IDI (Image Diversity Index).

$$IDI'_c = - \sum_{i=1}^S pi * \ln pi$$

where,

S = number of image classes (43),

pi = proportion of vignettes belonging to class i to the total number of vignettes (277,481).

Table 5. The 43 plankton categories used to infer the class diversity index.

<b>Plankton categories used to infer the class diversity index</b>		
<i>Appendicularia</i>	<i>Ascidiacea</i>	<i>Bacillariophyceae</i>
<i>Bivalvia</i> < <i>Mollusca</i>	<i>Calanoida</i>	<i>Ceratium furca</i>
<i>Ceratium fusus</i>	<i>Ceratium</i>	<i>Chaetoceros sp.</i>
	<i>macroceros</i>	
<i>chaetoceros-like</i>	<i>Chaetognatha</i>	<i>Cirripedia</i>
<i>Cladocera</i>	<i>Collodaria</i>	<i>Copepoda</i>
<i>Corycaeus sp.</i>	<i>Coscinodiscus</i>	<i>Dinophyceae</i>
	<i>sp.</i>	
<i>Ditylum sp.</i>	<i>egg</i> < <i>Acartia</i>	<i>egg</i> < <i>Crustacea</i>
<i>egg</i> < <i>Teleostei</i>	<i>Evadne spinifera</i>	<i>Favella sp.</i>
<i>Gastropoda</i> < <i>Mollusca</i>	<i>Hydrozoa</i>	<i>Macrosetella</i>
		<i>gracilis</i>
<i>nauplii</i> < <i>Calanoida</i>	<i>nauplii</i> < <i>Copepod</i>	<i>nauplii</i> < <i>Cyclopoid</i>
	<i>a</i>	<i>a</i>
<i>nauplii</i> < <i>Temora</i>	<i>Noctiluca</i>	<i>Oithona sp.</i>
	<i>scintillans</i>	
<i>Oithona hebes</i>	<i>Oncaea sp.</i>	<i>Penilia avirostris</i>
<i>Polychaeta</i>	<i>Protoperidinium</i>	<i>Pyrocystis sp.</i>
	<i>sp.</i>	
<i>rhizosolenia-like</i>	<i>Temora turbinata</i>	<i>Tintinnida</i>
<i>Trichodesmium</i>		
<i>sp.</i>		

## CHANGE IN THE ASSEMBLAGE DIVERSITY

The diversity of image classes varied over time between 0,38 e 2,04 ( $\pm 0,28SD$ ) bits.class<sup>-1</sup>. The average was close to 1.41 and remained constant over time. High variations were observed between months and between years. Despite the high internal variability of the data, there is an apparent cycle of high diversity with an interval of about three years, as observed in 1999, 2001, 2004, 2007, 2011 (Figure 13).

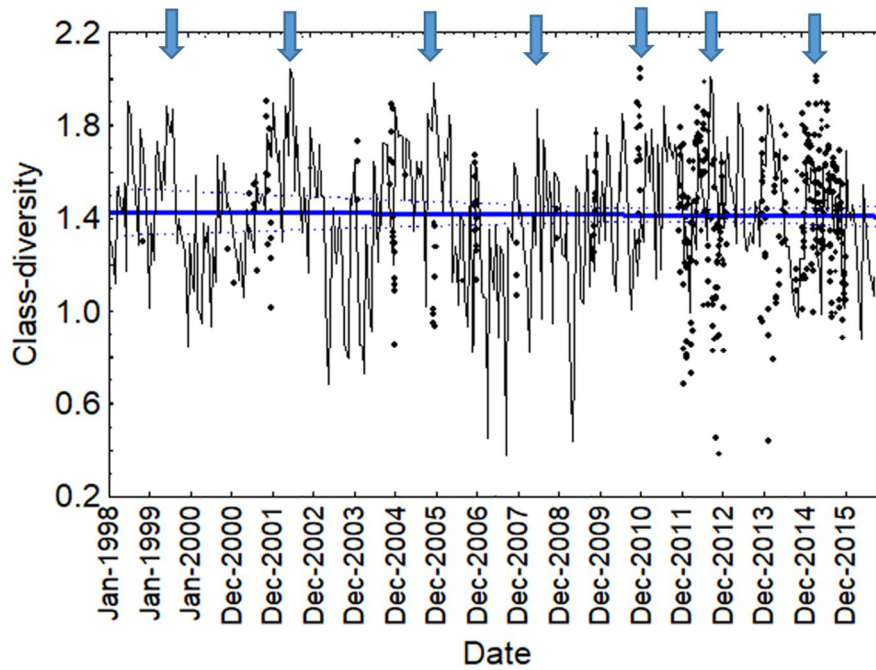


Figure 13. Estimated monthly variation between 1998 and 2015 in plankton class diversity. The blue arrows represent peaks of high diversity.

The annual average hides the monthly peaks shown above. However, it does suggest a correlation between temperature peaks and diversity peaks (Figure 14), but not with salinity (Figure 15). Between 1999 and 2002 there is an annual increase in temperature that is accompanied by an increase in diversity. After 2002 and until 2011, there seems to be a gradual decline in both parameters, interrupted in 2009 by a peak. After 2011, the temperature continues to drop, while diversity increases.

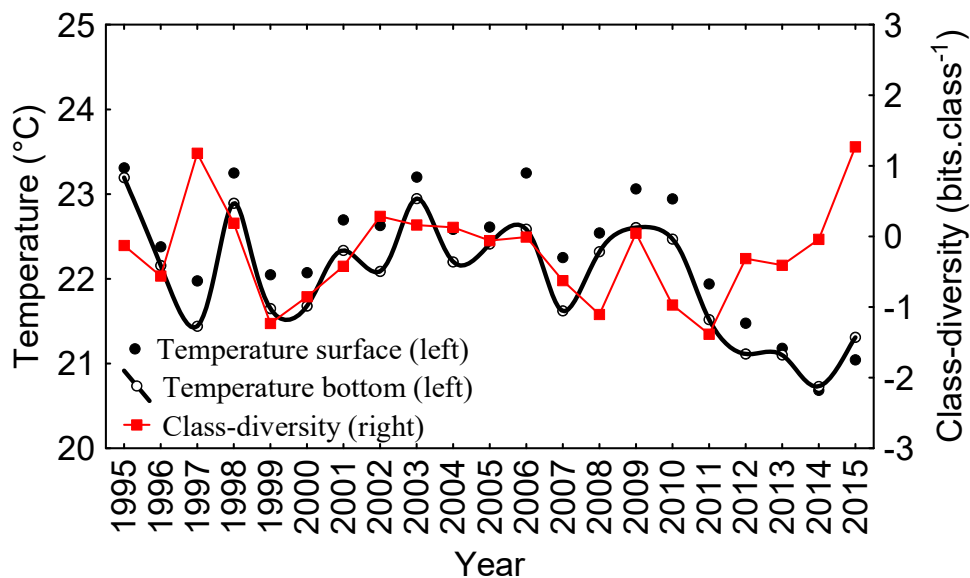


Figure 14. Annual average temperature variation (solid circles = surface; empty circles = background) and average class diversity.

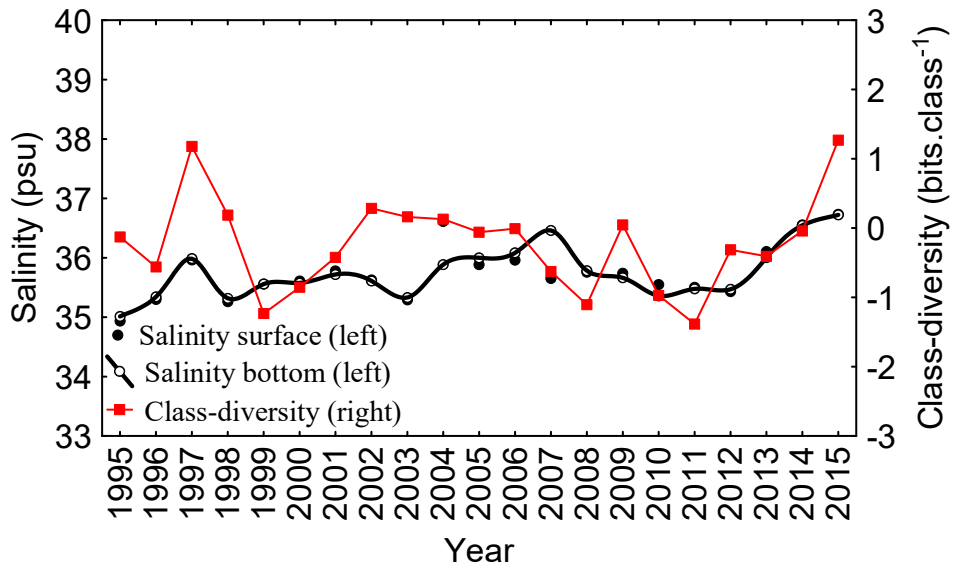


Figure 15. Annual mean salinity variation (solid circles = surface; empty circles = bottom) and mean class diversity.

Grouped every year, there is a period of greater diversity of classes in the months of May (5) to July (7), followed by a period of cava in the month of September. The high variability in the months of January, February, March, November and December suggest relevant interannual differences (Figure 16).

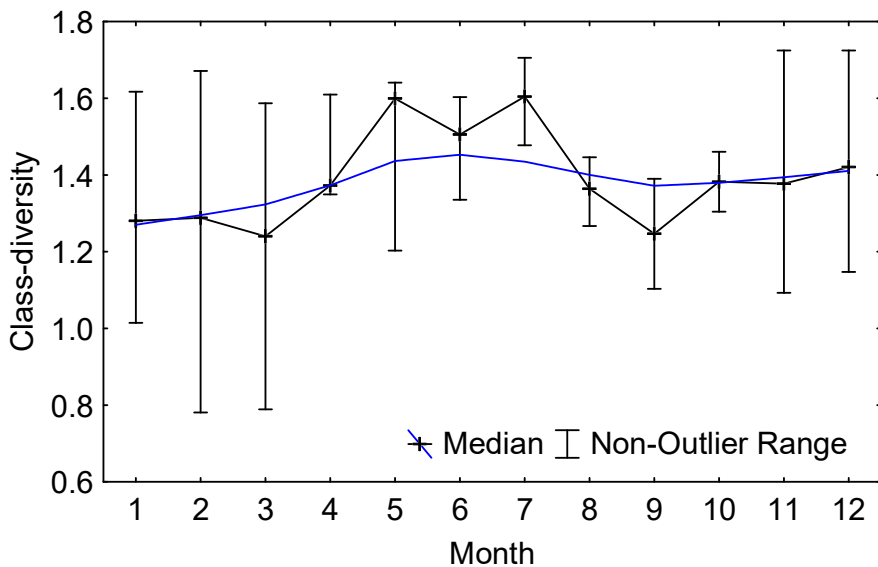


Figure 16. Monthly change in plankton class diversity calculated for the pooled months from 1998 to 2015.

**DISCUSSION**

The proposal of a new diversity index, applied to plankton images, aims to use the images in classes instead of species. Some works evaluate biodiversity based only on the number of species, using richness as a predictor variable, and not interspecific distinction (CADOTTE 2011; ROSCHER *et al.* 2012).

The knowledge of biological diversity allows to understand the spatial-time distribution of organisms in different environments (MAGURRAN, 2004), making it possible to assess the status of different ecosystems (MAGURRAN, 2004; SANTANA *et al.*, 2017)

Shannon's index assumes that, during random sampling for an infinite biocenosis, all species are sampled. Therefore, the sampling correlation is positive, that is, the number of different classes of plots increases as the distribution of areas between different classes of plots becomes equitable (KREBS, 2013; MAGURRAN, 2011).

The Shannon-Wiener index (SHANNON & WEAVER, 1949) is derived from information theory and has units that vary according to the logarithmic base used: bits, nats, or decits for base 2, neperian, and 10, respectively. The index, therefore, is difficult to interpret, but it can be understood as the degree of uncertainty in predicting to which species an individual, chosen at random from a sample with S species and N individuals, will belong (URAMOTO *et al.* 2005). Or it could be interpreted using H' as the improbability of a sequence of individuals randomly taken from the community to coincide with a predetermined sequence of species (MARTINS & SANTOS 1999).

The Shannon index is still the most used in ecology to estimate diversity, it was independently presented in ecology by (MARGALEF 1956) and (MACARTHUR 1955). In recent years, several diversity indices have been created, but none to work with ECOTAXA images. The Shannon index is widely used to quantify species diversity or richness in a community. It considers both the relative abundance of species and equitability, that is how species are distributed in terms of their abundance. The formula for calculating the Shannon index is as follows:

$$H = -\sum(\pi_i * \ln(\pi_i))$$

Where:

“H” represents the Shannon index.

$\pi_i$  is the proportion or relative frequency of a given species in relation to the total number of individuals or samples in the community.

$\ln(\pi_i)$  is the natural logarithm of  $\pi_i$ .

$\sum$  represents the sum over all species present in the community.

The maximum diversity of copepods according to the predictions of (MARGALEF, 1995) and (BOLTOVSCOY, 1981), is considered lower on the coast than in the more oceanic regions and minimum in the estuary

As in other studies on marine zooplankton (AVILA, T. R. 2009; BRADFORD-GRIEVE *et al.*, 1999; CAVALCANTI & LARRAZABÁL, 2004), the organisms of the Copepoda group are responsible for the greatest diversity, represented mainly by species of the Order Calanoida.

Evaluating the diversity of organisms in relation to temperature is one of the most important abiotic factors, according to ESTEVES (1988), water temperature influences biological processes, therefore an essential parameter to be analyzed.

According to AVILA, T. R. (2009) the distribution of Cladocera is related to lower salinities, indicating a greater influence of estuarine waters on the coast.

The new diversity index applied to the ECOTAXA images has similar mathematics to the Shannon index, but instead of using the number of species, it uses the number of vignettes in the ECOTAXA. As it is not possible to always establish by species, varying between family, genus and species, the unit used was the OTU - Operational Taxonomic Unit.

## **ACKNOWLEDGMENTS**

We are grateful to the IEAPM/Brazilian Navy and all those who have worked on the sampling and laboratory analysis, mainly the Chemical Group of IEAPM. Financial support to the development of this study was provided by the “Upwelling Long-Term Ecological Research” (PELD-RECA) (Proc. 441525/2016-4) and the “EU Horizon 2020 Mission Atlantic” (Grant Agreement No 862428) programs.

## **CONFLICT OF INTEREST**

The authors declare that they have no known competing financial interests or personal relationships that could have appeared to influence the work reported in this paper.

## **REFERENCES**

Ataky, S. T. M. & Lameiras Koerich, A. (2022). A novel bio-inspired texture descriptor based on biodiversity and taxonomic measures. *Pattern Recognition*, 123, 108382. doi: <https://doi.org/10.1016/j.patcog.2021.108382>.

Beardall J., Allen D., Bragg J., et al. Allometry and stoichiometry of unicellular, colonial and multicellular phytoplankton, *New Phytol.*, 2009, vol. 181 doi: 10.1111/j.1469-8137.2008.02660 [Google Scholar](#) [WorldCat](#)

Behrenfeld MJ, Randerson JT, McClain CR, Feldman GC, Los SO, et al. 2001. Biospheric primary production during an ENSO transition. *Science* 291:2594–97

Cadotte MW (2011) The new diversity: management gains through insights into the functional diversity of communities. *Journal of Applied Ecology* 48:1067-1069 DOI: 10.1111/j.1365-2664.2011.02056.x

Dias, C. O.; Bonecker, S. L. C. Long-term study of zooplankton in the estuarine system of Ribeira Bay, near a power plant (Rio de Janeiro, Brazil). *Hydrobiologia*, v. 614, p. 65-81, 2008. D.O.I.10.1007/s10750-008-9537-3

Magurran, A., 2002. *Measuring Biological Diversity*. Blackwell Science, Oxford.

Magurran, Anne E. *Measuring biological diversity*. *African journal of aquatic science*, v. 29, n. 2, p. 285-286, 2004.

McArthur, R.H. (1955) Fluctuations of animal populations, and a measure of community stability. *Ecology*, 36: 533-36.

Krebs, C. J. *Ecological methodology*. New York, Harper & Row, USA, 2013.

Margalef, R. (1956) Información y diversidad específica en las comunidades de organismos. *Invest. Pesq.*, 3: 99-106.

Martins F.R., Santos F.d. 1999. Técnicas usuais de estimativa da biodiversidade. *Revista Holos*. 1:236-267.

Picheral, M.; Colin, S.; Irisson, J.O. EcoTaxa—A Tool for the Taxonomic Classification of Images. 2017. Available online: <http://ecotaxa.obs-vlfr.fr/> (accessed on 10 July 2023).

R Core Team. 2008. *R: A language and environment for statistical computing*. R

- Foundation for Statistical Computing. Retrieved from <http://www.r-project.org>.
- Richardson, A.J. In hot water: zooplankton and climate change. – ICES Journal of Marine Science, v.65: p.279-295, 2008.
- Roscher C, Schumacher J, Gubsch M, Lipowsky A, Weigelt A, Buchmann N, Schmid B, Schulze E (2012) Using plant functional traits to explain diversity–productivity relationships. PLoS ONE 7:1:11 doi:10.1371/journal.pone.0036760
- Santana, L.M., L.O. Crossetti & C. Ferragut, 2017. Ecological status assessment of tropical reservoirs through the assemblage index of phytoplankton functional groups. Brazilian Journal of Botany 40: 695-704.
- Sieburth J. M., Smetacek V., Lenz J.. Pelagic ecosystem structure: heterotrophic compartments of the plankton and their relationship to plankton size fractions, *Limnol. Oceanogr.*, 1978, vol. 23 (pg. 1256 -1263) [Google Scholar](#) [Crossref](#) [WorldCat](#)
- Shannon, C.E. & Weaver, W. 1963. The mathematical theory of communication. Illinois University Press, Urbana.
- Sieracki, C., Sieracki, M.E., Yentsch, C., 1998. An imaging-in-flow system for automated analysis of marine microplankton. Marine Ecology Progress Series, 168, 285-296.
- Uramoto K., Walder J.M., Zucchi R.A. 2005. Análise quantitativa e distribuição de populações de espécies de *Anastrepha* (Diptera: Tephritidae) no campus Luiz de Queiroz, Piracicaba, SP. Neotropical Entomology. 34:33-39.
- University of Illinois. Silva E.A.d. 2014. Interações multitróficas no cerrado: resultados condicionais nas relações entre plantas, herbívoros e predadores Uberlândia: Universidade Federal de Uberlândia.

### CAPÍTULO III

Artigo a ser submetido na revista: Journal of Plankton Research

#### **EARLY WARNING INDICATORS OF SHIFTS IN THE PLANKTON ASSEMBLAGE IN UPWELLING ECOSYSTEMS**

Thiago da Silva Matos<sup>1</sup>, Carolina Siqueira dos Reis<sup>1</sup>, Laura de Andrade Moura<sup>2</sup>, Andressa C de Souza<sup>1</sup>, Ana Carolina Nogueira Luz<sup>1</sup>, Vanessa Trindade<sup>2</sup>, Yuri Artioli<sup>3</sup>, Guillem Chust<sup>4</sup>, Patrício Mariani<sup>5</sup>, Tania Ocimoto Oda<sup>2</sup>, Ricardo Coutinho<sup>1,2</sup>, Lohengrin Fernandes<sup>1,2</sup>

T.M.: [ORCID® 0000-0002-9390-7669](#)

C.R.: [ORCID® 0000-0003-1584-0988](#)

L.M.: [ORCID® 0000-0003-0002-9981](#)

A.S.:

A.C.L.: [ORCID® 0000-0002-6409-4021](#)

V.T.:

G.C.: [ORCID® 0000-0003-3471-9729](#)

P.M.:

T.O.: [ORCID® 0000-0003-4594-9562](#)

R.C.: [ORCID® 0000-0001-5430-2176](#)

L.F.: [ORCID® 0000-0002-8579-2363](#)

1 'Marine Biotechnology' Graduate Program IEAPM/UFF, Instituto de Estudos do Mar Almirante Paulo Moreira (IEAPM), Arraial do Cabo, Rio de Janeiro, Brazil

2 Instituto de Estudos do Mar Almirante Paulo Moreira (IEAPM), Arraial do Cabo, Rio de Janeiro, Brazil

3

4 AZTI Marine Research, Basque Research and Technology Alliance (BRTA), Txatxarramendi Ugarteia z/g, 48395 Sukarrieta, Spain

5

\*Corresponding author: [biologo.thiagomatos@gmail.com](mailto:biologo.thiagomatos@gmail.com)



## **Abstract**

Marine biodiversity is mainly composed of phytoplankton and zooplankton, with a wide variety of species of different sizes and shapes, which can be indicators of climatic and oceanic events. Researching and monitoring these organisms in a long-term help to understand the interaction and heterogeneity of species and to determine trends in the complex ecosystems to which they are associated, especially in areas of upwelling, as shown by previous studies on the role of plankton in the Cabo Frio Upwelling System (CFUS). Therefore, our aim was to find empirical evidence derived from temporal variability in planktonic assemblages to potentially indicate regime changes in CFUS, considering a series of more than 15 years of data on biotic and abiotic variables. The study had two premises: to analyze the decadal change in temperature and salinity along the CFUS, and then to evaluate if the biotic (planktonic) variables were correlated with the abiotic ones, in order to detect breakpoints and changes in the ecosystem in the study area. The study was carried out at a fixed station on Cabo Frio Island (23°S - 042.01°W), as part of the Long-Term Ecological Research (LTER). This island is in the center of the Cabo Frio Upwelling System (CFUS), a well-known wind-driven coastal upwelling on the west coast of the South Atlantic Ocean. For organisms counting, a Benchtop B3 FlowCAM cytometer was used, and the images were captured at a resolution of 2400 dpi. The annual averages of the different phytoplankton and zooplankton variables were highly correlated. Copepods, for example, had the highest variance inflation factor and were highly correlated with dinoflagellates (-0.83) and Chlorophyll-a (-0.56). The shift from a diatom-dominant to a dinoflagellate regime indicates the distinct responses these organisms have to certain environmental conditions. Dinoflagellate species, unlike diatoms, are specialists in ecosystems with higher salinity and temperature and low concentrations of nutrients. Unlike the zooplankton groups – copepods and cladoceras – they are considered opportunistic types of phytoplankton that tend to abrupt changes in ecosystems such as CFUS.

**Keywords:** Temporal changes, plankton, indicator, ecosystem shift, Cabo Frio Upwelling System

## **INTRODUCTION**

The South Atlantic Ocean is surrounded by 24 coastal countries members of the Zone of Peace and Cooperation of the South Atlantic (ZOPACAS) and provides several ecosystem services to nearly 840 million people living in South America and Africa (United Nations, 2021b). In its southernmost portion, down to  $\sim 20^{\circ}\text{S}$  on both sides (Figure 1), there are highly-productive areas, namely the Benguela Current System on the east (HUTCHINGS *et al.*, 2009) and the southwest South Atlantic Ocean (SWAO) on the west (FRANCO *et al.*, 2020; GIANELLI *et al.*, 2023), where large stocks of anchovies (*Engraulis anchoita*) and sardines (*Sardinella brasiliensis*) are overexploited through the years and threatened by hydroclimatic changes and ecosystem degradation (BERTRAND *et al.*, 2018). Several international agencies, multi-national organizations and scientific cooperations have warned on the risk of stock depletion if the ability of fishery management and monitoring fails (e.g. BARANGE *et al.*, 2018; FRANCO *et al.*, 2020; UNITED NATIONS, 2021). Besides fishery, most comprehensive models predicting the sustainability of these stocks over time claim spawning and recruitment as key drivers, as both depend on lower trophic levels (i.e. phytoplankton and zooplankton) as food supply (BEAUGRAND *et al.*, 2003; BEAUGRAND, 2005; LEES *et al.*, 2006).

Additionally, phytoplankton and zooplankton are key contributors to biodiversity, consisting of a wide variety of species, in different shapes and sizes, and being indicators of multiscale ocean and climatic events (LOMBARD *et al.*, 2019). A better understanding of primary and secondary production at specific regions requires access to consistent, high-quality, near real-time monitoring data on a series of climate, environmental and biological parameters (MILOSLAVICH *et al.*, 2018). Long-term research on these organisms can help understand species interaction and heterogeneity, to better determine trends in the complex ecosystems they are associated with (KLÉPARSKI *et al.*, 2022), as well as sentinels of early detection of global warming effects (BEAUGRAND and KIRBY, 2018a; CHUST *et al.*, 2023). Studies about plankton communities have increased over decades and are expected to continuously grow during the Ocean Decade, reinforcing its relevance to the scientific knowledge of the marine environment (SOUZA *et al.*, 2018; RYABININ *et al.*, 2019).

Abrupt changes can occur in plankton assemblages between system states, whether caused by global climate change, biological interactions or local environmental conditions (BODE, 2023).

Apart from collecting samples of these organisms, it is important to consider other abiotic/environmental variables for modelling their responses and suitability to events

(BEAUGRAND and KIRBY, 2018b). Ecosystems such as CFUS are highly dynamic and support the natural variability usually found in upwelling regions (CAPONE and HUTCHINS, 2013). Nevertheless, the hydrodynamic changes over decades in the CFUS, like the increasing flow of the Brazilian current (COELHO-SOUZA *et al.*, 2012), are thought to cause shifts in primary production, fish yields, and nutrient gain and loss. Whether these shifts are low-frequency, high-amplitude, and concurrent with changes in the hydroclimate system that propagate through several trophic levels to represent regime shifts in the ecosystem – according to the definition revised by (LEES *et al.*, 2006) – or natural variability is still under debate.

Previous studies have shown the role of plankton in the CFUS (e.g. GONZALEZ-RODRIGUEZ *et al.*, 1992; GONZALEZ-RODRIGUEZ, 1994; FERNANDES *et al.*, 2012; KÜTTER *et al.*, 2014). We, therefore, aimed at finding empirical evidence derived from the temporal variability in the planktonic assemblages to anticipate/indicate potential regime shifts in the Cabo Frio Upwelling System, considering a series of over 15 years of data on biotic and abiotic variables. First, the study aims at analyzing the decadal change in temperature and salinity (other abiotic parameters) over the CFUS. Then, the biotic (planktonic) variables were correlated to the abiotic ones to detect breakpoints and ecosystem shifts that occurred in the study area.

## **MATERIAL AND METHODS**

### ***Study site***

The present study was conducted in a fixed station in Cabo Frio Island (23°S - 042.01°W, Figure 1, red circle) as part of the Long-term Ecological Research (LTER) “Upwelling” Project (PELD-RECA, [cnpq.br/sites-peld](http://cnpq.br/sites-peld)), where the potential decadal oscillation in the upwelling effects upon the planktonic assemblages are expected to be stronger (COELHO-SOUZA *et al.*, 2012). This island is located at the center of the Cabo Frio Upwelling System (CFUS), a well-known coastal wind-driven upwelling on the western coast of the South Atlantic Ocean (Figure 1). Apart from the more stable northern subtropical pelagic ecosystem, this region has strong seasonality in the environment, the water temperature ranging from less than 15°C in the austral spring-summer (September-January) to more than 28°C during the autumn (March-April) (VALENTIN, 2001). The CFUS marks the north boundary of the South Brazilian Shelf (SBS) region (Figure 17).

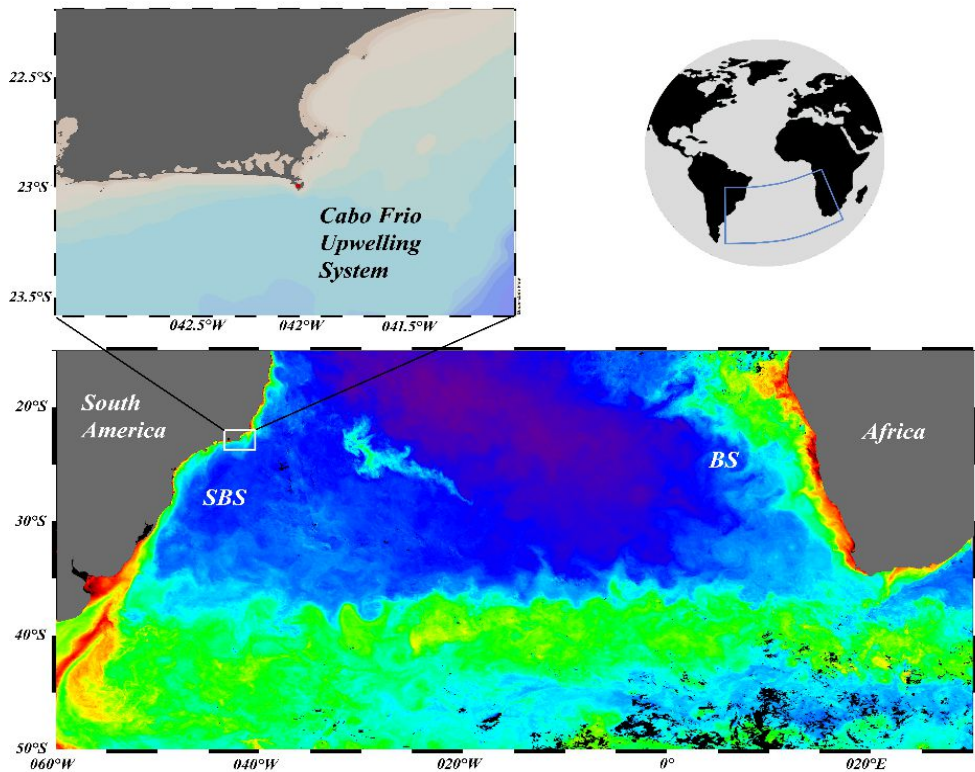


Figure 17. Monthly composite Chlorophyll concentration (MODIS Aqua L3 4km resolution) in the South Atlantic Ocean during January 2003 (Ocean Color, NASA). The Cabo Frio Upwelling System (CFUS, top panel) delimits the northern boundary of the South Brazilian Shelf in the southwestern South Atlantic Ocean (SWAO), a highly-productive ecosystem on the west that contributes to the South Atlantic primary production along with the Benguela System (BS) on the east.

To follow the temporal oscillations in the climate and the ecosystem status, this site has been weekly monitored since October 1994. The analysis of the environmental variables, namely water temperature, salinity, dissolved oxygen, and pH, was performed using either an inverted thermometer mounted on a Niskin bottle (1998 – 2012) or a Horiba multiparameter probe (Model U-5000; HGS No. 7JETA790) at ~1-m depth (2012 to date). Additionally, sub-superficial water samples of 2 litres were collected with a 3-L Niskin bottle and immediately conducted to the laboratory for spectrophotometric (Agilent UV-Vis Cary 60) estimates of the nutrient concentration (nitrite, nitrate, ammonia, and phosphate) (STRICKLAND and PARSONS, 1972).

The temporal change in the community structure was addressed by six biotic variables, including four estimates of the density of the dominant plankton groups (diatoms, dinoflagellates, cladocerans, and copepods) and two estimates of biomass (Chlorophyll-a and seston dry weight). Chlorophyll-a (Chla) concentration ( $\mu\text{g/l}$ ) was estimated from a 0.5 to 1 L subsample filtered in GFF Millipore membrane and analyzed in

the spectrophotometer following Jeffrey-Humphrey equation (JEFFREY and WELSCHMEYER, 1997; RITCHIE, 2008).

Plankton samples were collected in triplicates every week by sub-superficial horizontal hauls (~1 m) lasting for 2 minutes with a cylindrical-conical net, 40 cm mouth opening, 100 µm mesh size, and equipped with a calibrated flowmeter (Model 2030R Mechanical Flowmeter, General Oceanics Inc., Miami, FL). Immediately after collection, samples were preserved in a 4% solution of formaldehyde (final concentration), diluted in seawater and buffered with 20 g/l of Sodium tetraborate. At the laboratory, samples were split with a Folsom Plankton Splitter (BOLTOVSKOY, 1981), one subsample was used for dry weight in a 0.0001 g precision scale (Shimadzu 82D) and another for organisms counting.

### ***Plankton image acquisition***

For organisms counting, we used a Benchtop B3 FlowCAM cytometer configured in autoimaging mode with 2x objective, 2000µm x 2000µm flow cell. Images were captured at 2400 dpi resolution, with a size of 1024 x 768 pixels, 17 frames per second (efficiency ~40%), and a flow rate of 10 ml/min. A magnetic stirrer was used to keep the particles in suspension and the subsample concentration homogeneous during the analysis. Sample run interruptions were set on 4,000 particles in total. Visual Spreadsheet Software (VSP), version 3.4.5 (FLUIDIMAGING TECHNOLOGIES, 2013), was used for prior analysis and measurement of organisms. After the run, the images were pre-treated to split each Region of Interest by using coupled Python and ImageJ software ('Analyse Particles' function) and uploaded to the Ecotaxa platform (<https://ecotaxa.obs-vlfr.fr/prj/6015>), where the classification of organisms was performed. In total, 108 categories were generated, including supra-specific taxa and particles (e.g., faeces, fibres). The density of large (>100 µm) phytoplankton and zooplankton populations were estimated as the density of the four most abundant functional categories in the CFUS, namely diatoms (mostly *Coscinodiscus* spp.), dinoflagellates (mostly *Ceratium* spp. and *Noctiluca* sp.), copepods and cladocerans (*Pseudevadne tergestina*, *Evadne spinifera*, *Podon polyphemoides*, and *Penilia avirostris*), avoiding rare groups and badly annotated images. Each subsample was run into triplicates totalling nearly 50 ml analyzed. Each count was converted to density (organisms per cubic meter of seawater, org/m<sup>3</sup>) after considering the volume imaged by the FlowCam, the

subsample dilution, the fraction of Folsom, and the total volume filtered by the net as estimated by the flowmeter (ÁLVAREZ *et al.*, 2011, 2014).

### ***Time series analyses***

The full dataset of physical, chemical, and biological variables estimated in the fixed station (LTER “Upwelling” Project) was averaged to the corresponding month and year from 1995 to 2015 to complete a ~20-year set. Samples from October 1994 to December 1994 were not included in the analysis, and those from 2002 and 2003 were missing. These missing values in the series were replaced by the local mean using the ‘*impute*’ function (Tidyverse package, R Core Team, 2020). To extend the time series to previous decades (before 1995) and also to a larger area in the north boundary of the South Brazilian Shelf, all data available in the National Oceanographic Database (BNDO, Brazilian Navy, <https://www.marinha.mil.br/chm/bndo>) between 20°S – 24°S and 040°W – 044°W (0 to 30 m depth) of sea surface temperature (N=9568) and salinity (N=2939) was included in the dataset and used to build a decadal grid (1' x 1', radius = 50, kriging method). These data were obtained through distinct methods over the years, including inverted thermometers mounted on Nansen bottles, bathythermographs, and CTD profiles (supplementary material). We standardized all data before analysis to reduce the bias effect due to the device used. To our knowledge, there is no available data on pH, dissolved oxygen, or nutrient concentration for the whole area and before 1995 that could be included in the time series analysis. The monthly average of temperature and salinity were pooled every 10 years to address the coherence and constancy of the seasonal cycle in the CFUS over decades. Due to the scarcity of data from the 1950s, the matrix of seasonality was built exclusively with the monthly averages of temperature and salinity (12 months) estimated between 1960 and 2019 (the last 6 decades). Potential changes in the frequency of interannual oscillation in temperature and salinity were checked by the univariate Morlet wavelet value, calculated as  $\varphi(t) = \exp\frac{-t^2}{2} \cos(5t)$  (TORRENCE and COMPO, 1998) using the ‘*wt*’ function (biwavelet package, R Core Team, 2020). We addressed coincident shifts in both series by calculating the coherence wavelet index (‘*wtc*’ function) and highlighting significant correlations between temperature and salinity oscillations.

Considering only the CFUS region, the most relevant variables among the eight abiotic variables measured since 1995 (water temperature, salinity, dissolved oxygen, pH, nitrite, nitrate, ammonia, and phosphate) were selected using a Principal Component Analysis (PCA) calculated over the 8 x 21 matrix of year anomaly using the 'pca' function (stats Package, R Core Team, 2020). The data was previously standardized (z-transformed) by the 'decostand' function (vegan package, R Core Team, 2020). Potential collinearity between variables was verified through Pearson's Product Moment correlation by the 'pairs.panels' function (psych package, R Core Team, 2020) and also through the Variance Inflation Factor (VIF) using 'vif' function (car package, R Core Team, 2020) (ZUUR *et al.*, 2010). Variables with a correlation higher than  $\pm 50\%$  and  $VIF > 3$  were excluded from the analysis. Potential covariance between the abiotic parameters and the community structure was addressed by the contingency table (8 physical-chemical variables x 6 biological variables). We used the contingency table to check for potential linear or unimodal relationships between the organisms' composition and the environmental variables through Redundancy Analysis ('rda' function) and Canonical Correspondence Analysis ('cca' function) respectively and thus selected the best-fit model as suggested by the inertia (LEGENDRE and LEGENDRE, 2012). The best model was detailed based on the forward selection of significant variables using the 'ordiR2step' function. The resultant type of relationship was used to address whether the potential regime shift is 'smooth', 'abrupt', or 'discontinuous' according to the classification proposed by (LEES *et al.* 2006). We assessed potential significant deviation from stability over the years through the linear regression breakpoint analysis (function 'breakpoints', package strucchange), and highlighted through the traffic light plot (function 'traffilight', IEAtools package).

## RESULTS

### ***Decadal change in temperature and salinity***

The Cabo Frio Upwelling System (CFUS) limits the north boundary of the South Brazilian Shelf (SBS) between 22°S – 24°S and 040°W – 044°W by creating a horizontal gradient (east-west) of temperature and salinity between relatively warm and salty water ( $T > 20^{\circ}\text{C}$ ,  $S > 36,4$ ) transported by the Brazilian Current (BC) and the relatively cold and fresh ( $T < 20^{\circ}\text{C}$ ,  $S < 36,4$ ) upwelled South Atlantic Central Water (SACW) (CASTRO *et al.*, 2006). The intensity of this gradient increased from the 70s to the 90s by warmer ( $> 29^{\circ}\text{C}$ ,

Figure 2A, yellowish tones) and more saline waters (>36 psu, Figure 18B, reddish tones). In parallel to the decadal change in the strength of the gradient, there was a westward displacement of the cold core of the upwelling in CFUS. The SACW upwelling is strong at Cabo Frio Island (Figure 18A, black circle), but its nucleus moved westward from the 80s to the 90s towards Guanabara Bay (Figure 18A, red arrow). Recently (2020-2023), the cold core has aroused back with high intensity near Cabo Frio Island.

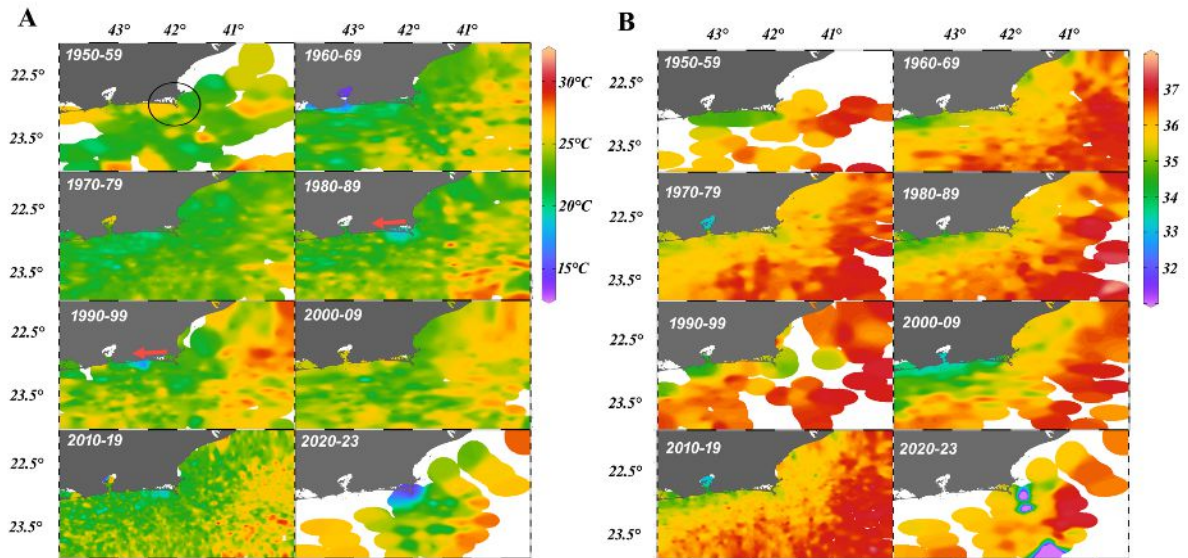


Figure 18. Decadal (1950-2023) change in the sea surface temperature (A) and salinity (B) in the CFUS.

Apart from the decadal changes, our results highlight the period of ~12 months (Figure 19A) as the most powerful oscillation of temperature in the CFUS lasting over decades that coincides with the full seasonal cycle (Figure 19D). A disruption in this rhythm was revealed at the end of the 70s and beginning of the 80s due to the occurrence of high-frequency disturbances (~3 months) in the temperature (Figure 19A). Differently from temperature, the strongest oscillation observed in the salinity before the 90s had a period lower than 6 months (Figure 19B). Apart from a weak seasonal oscillation in salinity before the 90s, there are no significant cycles of 12 months, and the average salinity equals 35.8 psu over the months (Figure 19E). By combining the time series (Figure 19C), it seems that the coherence between temperature and salinity time series is restricted to 12 months in the 70s and 4 months after the 00s. Our data suggest, therefore, that the seasonality in the thermo-haline regime was likely replaced by high-frequency oscillations (3-4 months period), mostly dictated by salinity (Figure 19E, black arrows to the left).



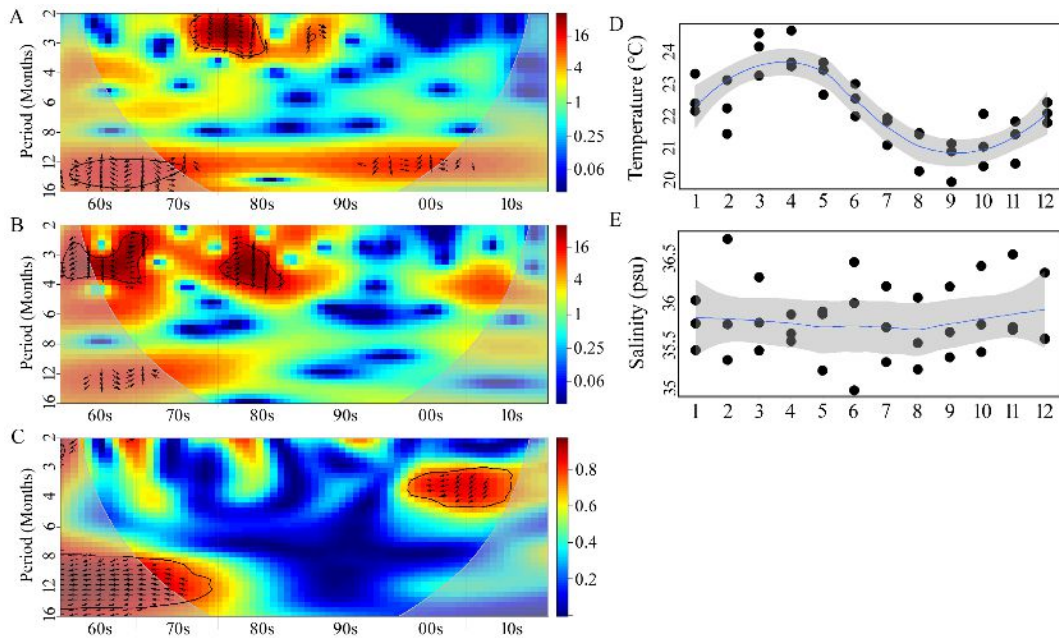


Figure 19. Wavelet transformation of temperature (A) and salinity (B), wavelet coherence (C), and monthly variation (seasonal) of temperature (D) and salinity (E) in the CFUS.

After the 90s, the interannual change in the temperature and salinity (Figures 20C and 20F) combined with the changes in the dissolved oxygen concentration represented the majority (34.2%) of the variance in the CFUS environment (Figure 20H). According to the first principal component, the environmental parameters can be summarized in two opposite trends over the years: decreasing temperature and increasing salinity/dissolved oxygen (Figures 20A, 20C, and 20F). The second orthogonal principal component describes 22.3% of the variance in the CFUS, likely related to the strong decrease in the concentration of nutrients ( $PO_4+NO_3+NO_2$ ) between 2002 and 2004 (Figures 20E and G).

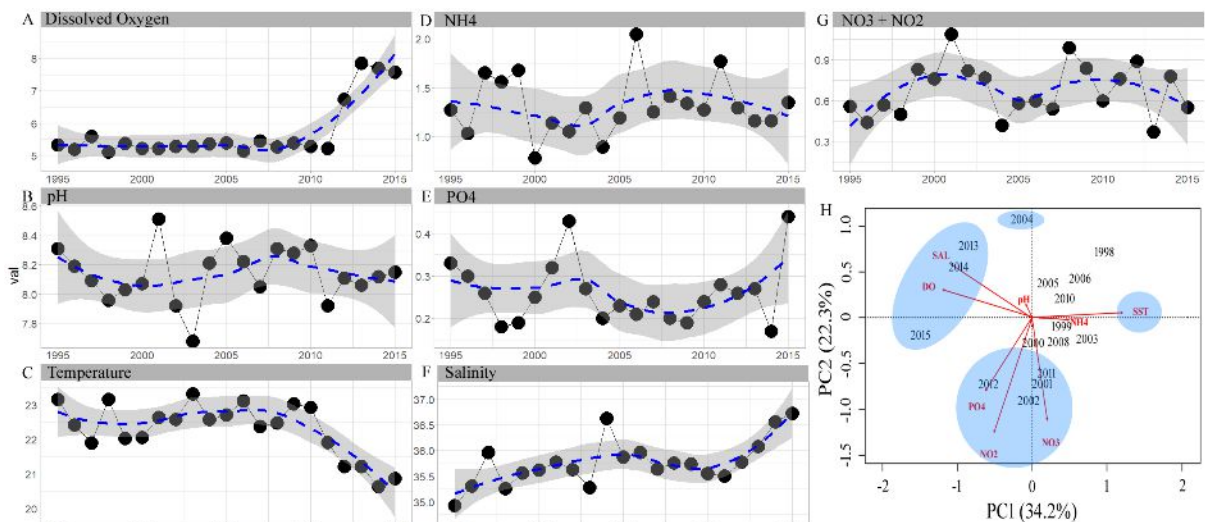


Figure 20. Annual average of dissolved oxygen (A), pH (B), temperature (C), ammonia (D), phosphate (E), salinity (F), nitrite+nitrate (G), and first two Principal Component axis.

### Temporal change in the plankton assemblage

The annual average of distinct phytoplankton and zooplankton variables were highly correlated (Figure 21). Copepods, for instance, had the highest variance inflation factor (Table 7) and were highly correlated to dinoflagellates (-0.83) and Chlorophyll-a (-0.56). After removing copepods from the matrix, all variables had VIF < 3 and thus were included in the model analysis.

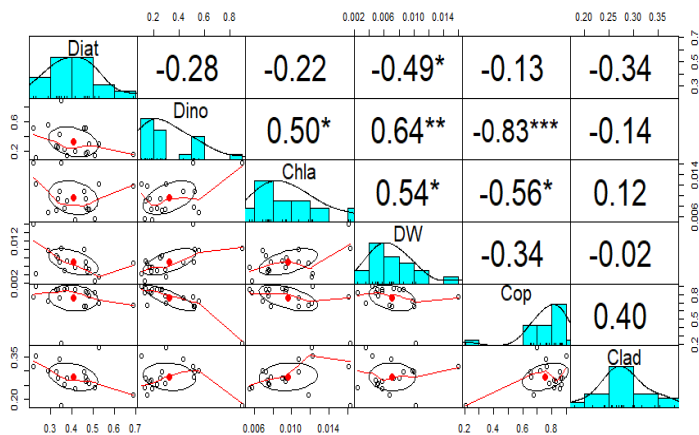


Figure 21. Scatterplots, histograms and correlation between the annual average of phytoplankton (Diatom, Dinoflagellates, and Chlorophyll-a) and zooplankton (Dry Weight, Copepod, and Cladoceran). \* $p < 0.05$ , \*\* $p < 0.01$ , \*\*\* $p < 0.001$ .

Table 6. Variance Inflation Factors (VIF) of variables included in the model before (Round 1) and after (Round 2) removal of collinearity.

	R	R
	ound 1	ound 2
Copep	8	re
od	.8	moved
Diato	4	2.
m	.6	3
Clado	4	2.
ceran	.2	1
Dry	2	1.

Weight	.4	9	
Dinofl		2	1.
agellate	.0	4	
Chloro		1	1.
phyll-a	.3	3	

---

The relationship between these physical-chemical variables and the spatial representation of biological variables follows a linear model (inertia = 2.96) rather than a Gaussian one (inertia = 0.07). The forward selection steps lead to the inclusion of all variables in the model, except for Copepoda ( $R^2_{\text{adjusted}} = 0.23$ ), thus the linear model produced by the redundancy analysis (RDA) explained the majority (69%) of the temporal variance of the 5 biotic variables selected in the round 2 (Table 7) relatively to the abiotic variables. The two most significant dimensions in the RDA explained 69% (38.9% + 30.4%) of the total variance observed in the ecosystem (Figure 21). The first dimension summarized 38.9% of the variance and pointed to a transition from a diatom-dominant to a dinoflagellate-dominant regime (Figure 21). This apparent regime shift is coincident with the rise in the relative abundance of cladocerans to copepods (Figure 22). The temperature was the only vector positively related to the first dimension, grouping those years before 2004, while nitrite, dissolved oxygen, and less pronounced phosphate, were negatively related. The nutrients and the dissolved oxygen that usually increase during cold upwelled waters deviated to the opposite side and positively correlated to the dinoflagellates and the seston biomass (dry weight), particularly during recent years. The salinity was the strongest vector on the second dimension, which in combination with nitrogen sources ( $\text{NO}_3 + \text{NH}_4$ ) correlates to the 2004 to 2008 variance of diatoms.

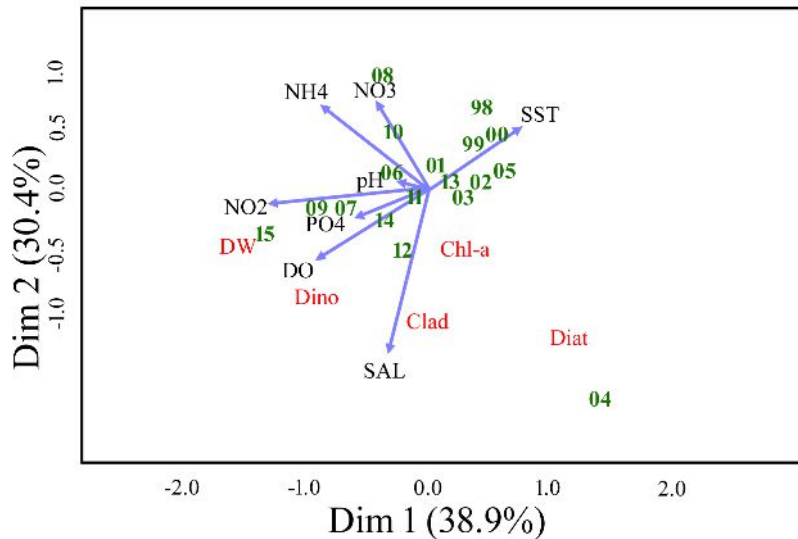


Figure 22. Scatterplot of dimensions 1 and 2 from the Redundancy Analysis in CFUS.

For most of the planktonic groups monitored, there was a peak in abundance during 2004 followed by a decrease up to 2008 (Figures 23 and 24). The peaks of Chlorophyll-a were likely due to increases in diatom abundance, and both time series exhibit the same general linear trend of decreasing in CFUS over the years. Dinoflagellates, in contrast, increased yearly, particularly after 2010. Copepods and cladocerans peaked in 2004 coincident with diatoms, but only cladocerans have an increasing trend over the years.

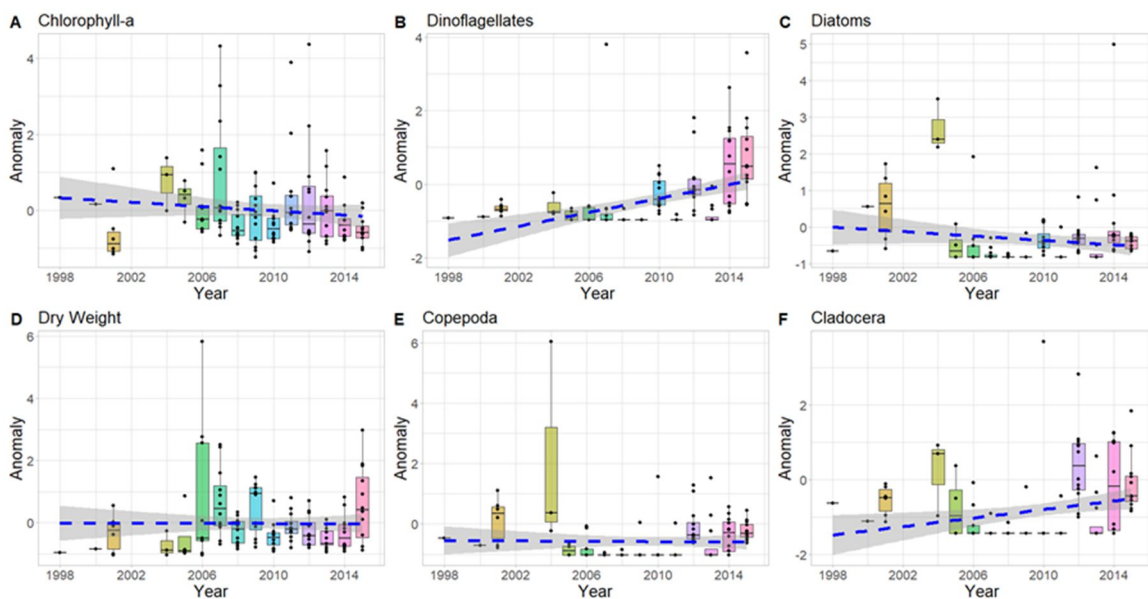


Figure 23. Annual average (horizontal line) of phytoplankton (A-C; Chlorophyll-a, Dinoflagellates, Diatoms) and zooplankton normalized-density (D-E; Dry Weight, Copepods, Cladocerans)  $\pm$  the 25th and 75th percentiles (lower and upper hinges respectively),  $\pm 1.5$ \* inter-quartile range (lower and upper whiskers respectively), raw data (black dots), and the linear model (dashed blue line).

When ranked by the likelihood of peaks (Figure 24), high densities of diatoms and copepods were more frequent during the first half of the time series. After 2004, the majority of the monthly average abundance of copepods and diatoms fell below 60% quintile. High abundances of dinoflagellates and cladocerans, in contrast, occurred more frequently during the second half of the time series. The representation of year scores in the first RDA dimension (Figure 24, blue line) illustrates the shift between regimes that coincided with the 2004 breakpoint.

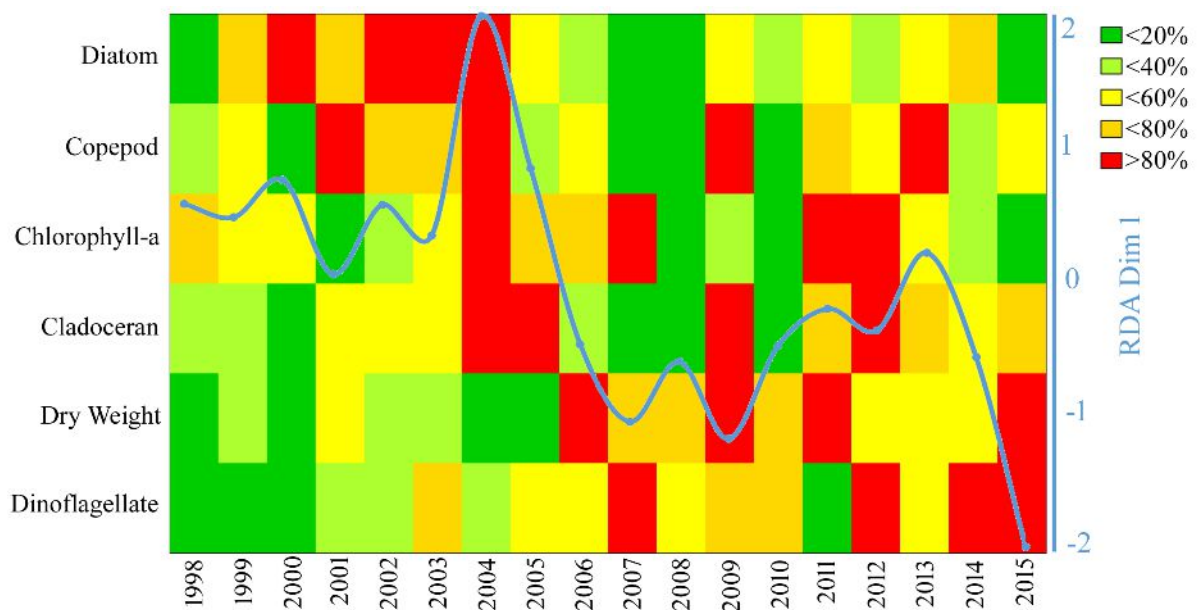


Figure 24. Ranked yearly distribution of quintiles of phytoplankton and zooplankton data (coloured scale) with superimposed scores of years in the first dimension of RDA (scales on the right).

## DISCUSSION

The Cabo Frio Upwelling System (CFUS) marks the limits between the South and East Brazilian Shelves. As a transient ecosystem in the southwestern South Atlantic Ocean (SWAO), it is likely to happen a high temporal natural variability in the environment that hides the one associated with a non-natural regime shift. Nevertheless, the observed southward displacement of the cold core and the increase in the thermo-haline gradient coincided with the period of most significant changes in the micro- and mesoplankton assemblages of the CFUS ecosystem. There is additional evidence supporting a coincident increasing trend in the rainfall and air temperature after the 90s in the coastal region of the SWAO (PENNEREIRO and MESCHIATTI, 2018). The Brazilian Current is a major component of the Atlantic Meridional Overturning Circulation in the region. A

warming of the Brazilian Current (BC) with shifts in the meandering behaviour over the past decades and combined with a poleward displacement in the CFUS NE/SW wind regime has been reported recently (CASTRO *et al.*, 2006). The warming region extends along the BC path, the South Brazilian Bight (~ 21° S–29° S) and the La Plata River (FRANCO *et al.*, 2020).

There are also additional reports highlighting the influence of the upwelling plumes on physical, chemical and biological conditions up to 400 km from CFUS (CASTRO *et al.*, 2006).

The natural seasonal oscillations of temperature, salinity, and nutrients are strong drivers of plankton phenology, fueling the spring bloom of phytoplankton, and signalling for spawning and hatching (JI *et al.*, 2010; FERNANDES *et al.*, 2012, 2017; LINDEMANN and JOHN, 2014). The observed weakening of seasonal oscillation in salinity since the 90s and increasing global trend might have intrinsic impacts on organisms' physiology while are also expected to propagate across the trophic interconnections (JI *et al.*, 2010).

Differently from most of the South Brazilian Shelf, where the seasonal variability in plankton assemblage is driven by increases in the riverine runoff during the rainy season, the CFUS is predominantly influenced by seasonal and inter-annual variability in the oceanic and shelf waters intrusions (MARCOLIN *et al.*, 2014). The warm Tropical Water (TW) at the surface in the SBS results from high irradiance and evaporation rates, increasing temperature, salinity and vertical stratification. Under this stratified and oligotrophic regime of the TW, the plankton assemblage is highly diverse in species, but size-dominated by small organisms of pico- and nanoplankton. The first dimension in the RDA reflected this seasonal regime that groups all years before 2004 positively correlated with temperature, and negatively with nitrite and phosphate. In 2004, there was a sudden change towards the negative correlation between salinity and nitrogen (nitrate+ammonia) concentration.

The negative correlation with the first dimension describes the occasional deepening in the mixed layer due to the rise of the cold nutrient-rich South Atlantic Central Water (SACW) that brings new nutrients (PO<sub>4</sub> and NO<sub>2</sub>) and fuels primary production at the surface, cascading up to larger micro- and mesoplankton species.

The shift between a diatom-dominant regime to a dinoflagellate one indicates the distinct responses these organisms have to certain environmental conditions. Dinoflagellate species, in contrast to diatoms, are specialists in ecosystems with higher salinity and temperature rates and low nutrient concentrations (IRWIN *et al.*, 2012).

Differently from the zooplankton groups – copepods and cladocerans – they are considered opportunistic types of phytoplankton that have tendencies to abrupt shifts in ecosystems such as the CFUS (CAEL *et al.*, 2021).

### **ACKNOWLEDGMENTS**

We are grateful to the IEAPM/Brazilian Navy and all those who have worked on the sampling and laboratory analysis, mainly the Chemical Group of IEAPM.

### **FUNDING**

This project has received funding from the European Union's Horizon 2020 research and innovation programme under Grant Agreement No 862428 (MISSION ATLANTIC). This output reflects only the author's view and the Research Executive Agency (REA) cannot be held responsible for any use that may be made of the information contained therein.

### **CONFLICT OF INTEREST**

The authors declare that they have no known competing financial interests or personal relationships that could have appeared to influence the work reported in this paper.

### **AUTHOR CONTRIBUTION**

T.M.: Formal Analysis; Investigation; Writing – review & editing;

C.R.: Sampling; Analysis, Investigation; Writing – original draft & editing;

L.M.: Formal Analysis; Investigation; Writing – review & editing;

A.S.: Formal Analysis; Investigation; Writing – review & editing;

A.C.L.: Sampling; Writing – review & editing.

V.T.: Formal Analysis; Investigation; Writing – review & editing;

Y.A.: Formal Analysis; Investigation; Writing – review & editing;

G.C.: Supervision; Resources; Writing – review & editing.

P.M.: Supervision; Resources; Writing – review & editing.

T.O.: Formal Analysis; Investigation; Writing – review & editing;

R.C.: Supervision; Resources; Writing – review & editing.

L.F.: Supervision; Resources; Writing – review & editing.

### **REFERENCES**



Álvarez, E., López-Urrutia, Á., Nogueira, E. & Fraga, S. 2011. How to effectively sample the plankton size spectrum? A case study using FlowCAM. *Journal of Plankton Research*, 33(7), 1119–1133. DOI: <https://doi.org/10.1093/plankt/fbr012>

Álvarez, E., Moyano, M., Lopez-Urrutia, Á., Nogueira, E., Scharek, R., López-Urrutia, Á., Nogueira, E. & Scharek, R. 2014. Routine determination of plankton community composition and size structure: a comparison between FlowCAM and light microscopy. *Journal of Plankton Research*, 36(1), 170–184. DOI: <https://doi.org/10.1093/plankt/fbt069>

Barange, M., Holsman, K., Hollowed, A., Ito, S., Bograd, S., Hazen, E., King, J., Mueter, F. & Perry, R. I. 2018. *Impacts of climate change on fisheries and aquaculture: synthesis of current knowledge, adaptation and mitigation options*. (Barange, M., Bahri, T., Beveridge, M. C. M., Cochrane, K. L., Funge-Smith, S., & Poulain, F., eds.), *FAO Fisheries and Aquaculture Technical Paper* (Vol. 627). Rome: FAO, 628pp pp.

Beaugrand, G. 2005. Monitoring pelagic ecosystems using plankton indicators. *ICES Journal of Marine Science*, 62(3), 333–338. DOI: <https://doi.org/10.1016/j.icesjms.2005.01.002>

Beaugrand, G., Brander, K. M., Lindley, J. A., Souissi, S. & Reid, P. C. 2003. Plankton effect on cod recruitment in the North Sea. *Nature*, 426(6967), 661–664. DOI: <https://doi.org/10.1038/nature02164>

Beaugrand, G. & Kirby, R. R. 2018a. How do marine pelagic species respond to climate change? Theories and observations. *Annual Review of Marine Science*, 10, 169–197. DOI: <https://doi.org/10.1146/annurev-marine-121916-063304>

Beaugrand, G. & Kirby, R. R. 2018b. How Do Marine Pelagic Species Respond to Climate Change? Theories and Observations. *Annual Review of Marine Science*, 10, 169–197.



Bertrand, A., Vögler, R. & Defeo, O. 2018. Climate change impacts, vulnerabilities and adaptations: Southwest Atlantic and Southeast Pacific marine fisheries. *In*: Barange, M., Holsman, K., Hollowed, A., Ito, S., Bograd, S., Hazen, E., King, J., Mueter, F., & Perry, R. I. (eds.), *Impacts of climate change on fisheries and aquaculture: synthesis of current knowledge, adaptation and mitigation options* (pp. 325–346). FAO Fisheries and Aquaculture Technical Paper.

Bode, A. 2023. Synchronized multidecadal trends and regime shifts in North Atlantic plankton populations. *ICES Journal of Marine Science*, (May), 1–12. DOI: <https://doi.org/10.1093/icesjms/fsad095>

Boltovskoy, D. 1981. *Atlas del zooplancton del Atlántico Sudoccidental y métodos de trabajo con el zooplancton marino*. Mar del Plata: Instituto Nacional de Investigación y Desarrollo Pesquero (INIDEP), 936 pp.

Cael, B. B., Dutkiewicz, S. & Henson, S. 2021. Abrupt shifts in 21st-century plankton communities. *Science Advances*, 7(44). DOI: <https://doi.org/10.1126/sciadv.abf8593>

Capone, D. G. & Hutchins, D. A. 2013. Microbial biogeochemistry of coastal upwelling regimes in a changing ocean. *Nature Geoscience*, 6(9), 711–717. DOI: <https://doi.org/https://doi.org/10.1038/ngeo1916>

Castro, B. M., Brandini, F. P., Pires-Vanin, A. M. S. & Miranda, L. B. 2006. Multidisciplinary Oceanographic Processes On the Western Atlantic Continental Shelf Between 4°N and 34°S. *In: The Sea* (Vol. 14).

Chust, G., Taboada, F. G., Alvarez, P. & Ibaibarriaga, L. 2023. Species acclimatization pathways: Latitudinal shifts and timing adjustments to track ocean warming. *Ecological Indicators*, 146(December 2022), 109752. DOI: <https://doi.org/10.1016/j.ecolind.2022.109752>

Coelho-Souza, S. A., López, M. S., Guimarães, J. R. D., Coutinho, R. & Candella, R. N. 2012. Biophysical interactions in the Cabo Frio upwelling system, southeastern Brazil. *Brazilian Journal of Oceanography*, 60(3), 353–365.

Fernandes, L. D. de A., Netto, E. B. F. & Coutinho, R. 2017. Inter-annual cascade effect on marine food web: A benthic pathway lagging nutrient supply to pelagic fish stock. *PLoS ONE*, 12(9), e0184512. DOI: <https://doi.org/10.1371/journal.pone.0184512>

Fernandes, L. D. de A., Quintanilha, J., Monteiro-Ribas, W., Gonzalez-Rodriguez, E. & Coutinho, R. 2012. Seasonal and interannual coupling between sea surface temperature, phytoplankton and meroplankton in the subtropical south-western Atlantic Ocean. *Journal of Plankton Research*, 34(3), 236–244. DOI: <https://doi.org/10.1093/plankt/fbr106>

Franco, B. C., Defeo, O., Piola, A. R., Barreiro, M., Yang, H., Ortega, L., Gianelli, I., Castello, J. P., Vera, C., Buratti, C., Pájaro, M., Pezzi, L. P. & Möller, O. O. 2020. Climate change impacts on the atmospheric circulation, ocean, and fisheries in the southwest South Atlantic Ocean: a review. *Climatic Change*, 162(4), 2359–2377. DOI: <https://doi.org/10.1007/s10584-020-02783-6>

Gianelli, I., Orlando, L., Cardoso, L. G., Carranza, A., Celentano, E., Correa, P., de la Rosa, A., Doño, F., Haimovici, M., Horta, S., Jaureguizar, A. J., Jorge-Romero, G., Lercari, D., Martínez, G., Pereyra, I., Silveira, S., Vögler, R. & Defeo, O. 2023. Sensitivity of fishery resources to climate change in the warm-temperate Southwest Atlantic Ocean. *Regional Environmental Change*, 23(2). DOI: <https://doi.org/10.1007/s10113-023-02049-8>

Gonzalez-Rodriguez, E. 1994. Yearly variation in primary productivity of marine phytoplankton from Cabo Frio (RJ, Brazil) region. *Hydrobiologia*, 294, 145–156.

Gonzalez-Rodriguez, E., Valentin, J. L., Andre, D. L. & Jacob, S. A. 1992. Upwelling and downwelling at Cabo Frio (Brazil): Comparison of biomass and primary production responses. *Journal of Plankton Research*, 14(2), 289–306. DOI: <https://doi.org/10.1093/plankt/14.2.289>

Hutchings, L., van der Lingen, C. D., Shannon, L. J., Crawford, R. J. M., Verheye, H. M. S., Bartholomae, C. H., van der Plas, A. K., Louw, D., Kreiner, A., Ostrowski, M., Fidel, Q., Barlow, R. G., Lamont, T., Coetzee, J., Shillington, F., Veitch, J., Currie, J. C. & Monteiro, P. M. S. 2009. The Benguela Current: An ecosystem of four components. *Progress in Oceanography*, 83(1–4), 15–32. DOI: <https://doi.org/10.1016/j.pocean.2009.07.046>

Irwin, A. J., Nelles, A. M. & Finkel, Z. V. 2012. Phytoplankton niches estimated from field data. *Limnology and Oceanography*, 57(3), 787–797. DOI: <https://doi.org/10.4319/lo.2012.57.3.0787>

Jeffrey, S. & Welschmeyer, N. 1997. Spectrophotometric and fluorometric equations in common use in oceanography. In: Jeffrey, S. W., Mantoura, R. F. C., & Wright, S. W. (eds.), *Phytoplankton Pigments in Oceanography: Guidelines to Modern Methods* (pp. 597–621). Paris: Unesco Publishing.

Ji, R., Edwards, M., Mackas, D. L., Runge, J. A. & Thomas, A. C. 2010. Marine plankton phenology and life history in a changing climate: current research and future directions. *Journal of Plankton Research*, 32(10), 1355–1368. DOI: <https://doi.org/10.1093/plankt/fbq062>

Kléparski, L., Beaugrand, G. & Kirby, R. R. 2022. How do plankton species coexist in an apparently unstructured environment? *Biology Letters*, 18, 20220207. DOI: <https://doi.org/10.1086/282171>

Kütter, V. T., Wallner-Kersanach, M., Sella, S. M., Albuquerque, A. L. S., Knoppers, B. A. & Silva-Filho, E. V. 2014. Carbon, nitrogen, and phosphorus stoichiometry of plankton and the nutrient regime in Cabo Frio Bay, SE Brazil. *Environmental Monitoring and Assessment*, 186, 559–573.

Lees, K., Pitois, S., Scott, C., Frid, C. & Mackinson, S. 2006. Characterizing regime shifts in the marine environment. *Fish and Fisheries*, 7, 104–127.

Legendre, P. & Legendre, L. 2012. *Numerical Ecology* (3rd ed.). Elsevier Academic Press, 1006 pp.

Lindemann, C. & John, M. A. St. 2014. A seasonal diary of phytoplankton in the North Atlantic. *Frontiers in Marine Science*, 1(SEP), 1–6. DOI: <https://doi.org/10.3389/fmars.2014.00037>

Lombard, F., Boss, E., Waite, A. M., Uitz, J., Stemmann, L., Sosik, H. M., Schulz, J., Romagnan, J. B., Picheral, M., Pearlman, J., Ohman, M. D., Niehoff, B., Möller, K. O., Miloslavich, P., Lara-Lopez, A., Kudela, R. M., Lopes, R. M., Karp-Boss, L., Kiko, R., Jaffe, J. S., Iversen, M. H., Irisson, J. O., Hauss, H., Guidi, L., Gorsky, G., Giering, S. L. C., Gaube, P., Gallagher, S., Dubelaar, G., Cowen, R. K., Carlotti, F., Briseño-Avena, C., Berline, L., Benoit-Bird, K. J., Bax, N. J., Batten, S. D., Ayata, S. D. & Appeltans, W. 2019. Globally consistent quantitative observations of planktonic ecosystems. *Frontiers in Marine Science*, 6(MAR). DOI: <https://doi.org/10.3389/fmars.2019.00196>

Marcolin, C. R., Gaeta, S. & Lopes, R. M. 2014. Seasonal and interannual variability of zooplankton vertical distribution and biomass size spectra off Ubatuba, Brazil. *Journal of Plankton Research*, 37(4), 808–819. DOI: <https://doi.org/10.1093/plankt/fbv035>

Miloslavich, P., Bax, N. J., Simmons, S. E., Klein, E., Appeltans, W., Aburto-Oropeza, O., Andersen Garcia, M., Batten, S. D., Benedetti-Cecchi, L., Checkley, D. M., Chiba, S., Duffy, J. E., Dunn, D. C., Fischer, A., Gunn, J., Kudela, R., Marsac, F., Muller-Karger, F. E., Obura, D. & Shin, Y. J. 2018. Essential ocean variables for global sustained observations of biodiversity and ecosystem changes. *Global Change Biology*, 24(6), 2416–2433. DOI: <https://doi.org/10.1111/gcb.14108>

Penereiro, J. C. & Meschiatti, M. C. 2018. Trends in the annual rainfall and temperatures series in Brazil. *Engenharia Sanitaria E Ambiental*, 23(2), 319–331. DOI: <https://doi.org/10.1590/S1413-41522018168763>

R Core Team. 2020. R: a language and environment for statistical computing. Vienna, Austria: R Foundation for Statistical Computing. Accessed: <https://www.r-project.org/>

Ritchie, R. J. 2008. Universal chlorophyll equations for estimating chlorophylls a, b, c, and d and total chlorophylls in natural assemblages of photosynthetic organisms using acetone, methanol, or ethanol solvents. *Photosynthetica*, 46(1), 115–126. DOI: <https://doi.org/10.1007/s11099-008-0019-7>

Ryabinin, V., Barbière, J., Haugan, P., Kullenberg, G., Smith, N., McLean, C., Troisi, A., Fischer, A. S., Aricò, S., Aarup, T., Pissierssens, P., Visbeck, M., Enevoldsen, H. & Rigaud, J. 2019. The UN decade of ocean science for sustainable development. *Frontiers in Marine Science*, 6(JUL). DOI: <https://doi.org/10.3389/fmars.2019.00470>

Souza, C. A., Gomes, L. F., Nabout, J. C., Velho, L. F. M. & Vieira, L. C. G. 2018. Temporal trends of scientific literature about zooplankton community Tendências temporais na literatura científica sobre a comunidade zooplanctônica. *Neotropical Biology and Conservation*, 13(4), 274–286. DOI: <https://doi.org/10.4013/nbc.2018.134.01>

Strickland, J. & Parsons, T. 1972. *A Practical Handbook of Seawater Analysis* (2nd ed.). Ottawa: Fisheries Research Board of Canada Bulletin 167, 310 pp.

Torrence, C. & Compo, G. P. 1998. A Practical Guide to Wavelet Analysis. *Bulletin of the American Meteorological Society*, 79(1), 61–78. DOI: <https://doi.org/10.4324/9780429311369-6>

United Nations. 2021a. The Second World Ocean Assessment II. Volume II. *Vol II, Chap. 20, II*, 520. Accessed: <https://www.un.org/regularprocess/woa2launch#>

United Nations. 2021b. *World Ocean Assessment II*. 570pp pp.

Valentin, J. L. 2001. The Cabo Frio Upwelling System, Brazil. *In*: Seeliger, U. & Kjerfve, B. (eds.), *Coastal Marine Ecosystems of Latin America* (Vol. 144, pp. 97–105). Springer Berlin Heidelberg. DOI: [https://doi.org/10.1007/978-3-662-04482-7\\_8](https://doi.org/10.1007/978-3-662-04482-7_8)

Zuur, A. F., Ieno, E. N. & Elphick, C. S. 2010. A protocol for data exploration to avoid common statistical problems. *Methods in Ecology and Evolution*, 1(1), 3–14. DOI: <https://doi.org/10.1111/j.2041-210x.2009.00001.x>

## CONSIDERAÇÕES FINAIS

O ecossistema marinho possui uma dinâmica muito diversificada em função de vários parâmetros bióticos e abióticos presentes, os organismos planctônicos contribuem para boa parte da diversidade biológica desse ambiente. Portanto monitorar a dinâmica desses organismos, biomassa, abundância e diversidade permite diagnosticar o status do ecossistema e assim prever algumas alterações futuras. No entanto estudar esses organismos por meio de imageamento possibilita resposta mais agilizada frente a alguma alteração desse ambiente. Neste trabalho podemos ver o desenvolvimento de um protocolo de contagem e classificação de imagens de plâncton, assim tratar imagens com ruídos no fundo.

Outra proposta deste trabalho, foi a elaboração de um novo índice de diversidade para ser aplicado em imagens previamente classificadas no ECOTAXA, ou qualquer outro site ou software de classificação de plâncton. Com a aquisição das imagens e tratadas nos programas, foi possível estabelecer a relação ecológica entre os organismos e os parâmetros ambientais, pode ser ressaltado nesse trabalho as mudanças de temperatura ao longo das décadas, a influência do fenômeno da ressurgência do Cabo Frio na distribuição, biomassa, e diversidade do plâncton.

Dessa forma, os estudos realizados neste trabalho evidenciam a importância da continuidade dessas pesquisas. Aperfeiçoar as técnicas existentes e desenvolver novas tecnologias, possibilitara melhor compreensão dos ecossistemas.

## REFERÊNCIAS BIBLIOGRÁFICAS

Bi, H., Guo, Z., Benfield, M. C., Fan, C., Ford, M., Shahrestani, S., & Sieracki, J. M., (2015). A semi-automated image analysis procedure for in Situ plankton imaging systems. PLoS ONE, 10(5), 1-17. <https://doi.org/10.1371/journal.pone.0127121>

Bonecker, S. L. C. Atlas de zooplâncton da região central da Zona Econômica Exclusiva brasileira. Rio de Janeiro: Museu Nacional, 2006. 232.

Bradford-Grieve, J. M.; Markhaseva, E.I.; Rocha, C. E. F., (1999). Copepoda. In: Boltovskoy, D. (Ed.). South Atlantic Zooplankton. Leiden. Backhuys Publishers, V. 2, p. 869-1098.

BOLTOVSKOY, D. Atlas del zooplancton del Atlántico Sudoccidental y métodos de trabajo con el zooplancton marino. Mar del Plata: Instituto Nacional de Investigación y Desarrollo Pesquero, 1981.

Calbet A., Trepát I., Almeda R., Saló V., Saiz E., Movilla J. I., Alcaraz M., et al. Impact of micro- and nanograzers on phytoplankton assessed by standard and size-fractionated dilution grazing experiments, Aquatic Microbial Ecology, 2008, vol. 50(pg. 145-156)

CORDEIRO, Tarcisio A.; BRANDINI, Frederico P.; MARTENS, Peter. Spatial distribution of the Tintinnina (Ciliophora, Protista) in the North Sea, spring of 1986. Journal of Plankton Research, v. 19, n. 10, p. 1371-1383, 1997.

Davis, C. S., Hu, Q., Gallager, S. M. *et al.* (2004) Real-time observation of taxa-specific plankton distributions: an optical sampling method. Mar. Ecol. Prog. Ser., 284, 77–96.

DANOVARO, R. et al. Marine viruses and global climate change. FEMS Microbiology Reviews, v. 35, p. 993–1034, 2011.

Grosjean, P., Picheral, M., Warembourg, C. *et al.* (2004) Enumeration, measurement and identification of net zooplankton samples using the ZOOSCAN digital imaging system. ICES J. Mar. Sci., 61, 518–525.



Gorsky, G., Ohman, M. D., Picheral, M. *et al.* (2010) Digital zooplankton image analysis using the ZooScan integrated system. *J. Plankton Res.*, 32, 285–303.

Gonzalez, R. C., Woods R. E., and Eddins S. L. (2004). *Digital Image Processing Using MATLAB*. Prentice Hall. pag. 72.

Harris, R. P.; Wiebe, P. H.; Lenz, J.; Skjoldal, H. R.; Huntley, M., (2000). *Zooplankton Methodology Manual*. Academic Press. 684p.

HIRST, A. G.; BUNKER, A. J. Growth of marine planktonic copepods: global rates and patterns in relation to chlorophyll a, temperature, and body weight. *Limnology and Oceanography*, v. 48, n. 5, p. 1988-2010, 2003.

Henzler, C.M., Hoaglund E.A., Gaines S. D., (2010). FISH-CS – a rapid method for counting and sorting species of marine zooplankton. *Marine Ecology Progress Series*, 410, 1-11.

Hirche, H. J., Schulz, J., & Hanken, T. (2012). A modular imaging system for collection and analysis of live and preserved zooplankton samples. *Program Book – OCEANS 2012 MTS/IEEE Yeosu: The Living Ocean Coast – Diversity of Resources and Sustainable Activities*.<https://doi.org/10.1109/OCEANS-Yeosu.2012.6263514>.

Luo, T., Kramer, K., Goldgof, D. B. *et al.* (2004) Recognizing plankton images from the shadow image particle profiling evaluation recorder. *IEEE Trans. Syst. Man Cyber. B*, 34, 1753–1762.

Schmid, M. S., Aubry, C., Grigor, J., Fortier, L. (2016). The LOKI underwater imaging system and an automatic identification model for the detection of zooplankton taxa in the Arctic Ocean. *Methods in Oceanography*. DOI: 10.1016/j.mio.2016.03.003.

Sosik, H. M. and Olson, R. J. (2007) Automated taxonomic classification of phytoplankton sampled with imaging-in-flow cytometry. *Limnol. Oceanogr. Meth*, 5, 204–216.

Tang, X., Stewart, W. K., Vincent, L. *et al.* (1998) Automatic plankton image recognition. *Artif. Intell. Rev.*, 12, 177–199.

Turner J. T. The importance of small planktonic copepods and their roles in pelagic marine food webs, *Zoological Studies*, 2004, vol. 43 (pg. 255-266)